UNIVERSITE JOSEPH KI-ZERBO

———

ECOLE DOCTORALE INFORMATIQUE

ET CHANGEMENTS CLIMATIQUES

BURKINA FASO

Unité-Progrès-Justice

MASTER RESEARCH PROGRAM

SPECIALITY: INFORMATICS FOR CLIMATE CHANGE (ICC)

MASTER THESIS

Subject:

Improving the quality of Gridded Precipitation Datasets over Burkina Faso Using merging Methods

by

Nabassebeguelogo Juste GARBA

Major Supervisor:

Prof. Tizane DHAO

Co-Supervisor:

Dr. Ulrich Jacques DIASSO

Academic year: 2021 - 2022

Dedication

To

Allah, for giving me the strength and blessing i needed to complete my Master's thesis.

My parents, who fought for my education, my brother for his encouragement and my wonderful wife, Balkissa, who had to endure my absences.

Acknowledgments

This thesis was made possible thanks to the contribution and help of several people who supported me morally, intellectually and materially. I am pleased to take this opportunity to express my sincere gratitude to:

- West African Science Service on Climate Change and Adapted Land Use (WASCAL) for providing this wonderful framework of capacity building.
- German Ministry of Education and Research (BMBF) for funding this program.
- Doctorate School of Informatics and Climate Change (ED-ICC) for explicitly organizing all related activities of the master's program in Informatics and Climate Change.
  - Prof. Tanga Pierre Zoungrana, the Director of ED-ICC,
  - Dr. Ousmane Coulibaly, the Deputy Director of ED-ICC,
  - and to ED-ICC staff members.
- Prof. Tizane DHAO, my major supervisor, for supporting my work with many contributions and guidelines.
- Dr. Ulrich DIASSO, my co-supervisor, for showing interest and guiding this research from its early stages until the completion of this document.
- Director General of the National Meteorological Agency, for giving permission to participate in this program.
- Lazare Sawadogo, the head of Climatology and Stations Network at the National meteorological Agency for the numerous contributions. He provided me with all the required support during my internship.
- The team of the Wascal competence center for the very rich exchanges and the advice. This team is made up of the following people: Dr Belko Abdoul Aziz Diallo, Dr Seyni Salack, Dr Oppong Hackman Kwame.
- Ousmane Ouedraogo, former database administrator of the National Meteorological Agency for giving me the first ideas on this work.
- Thanks to my colleagues and friend with whom I had a wonderful experience during the 2 years of the program.

Abstract

The management of climate risks such as droughts, floods and heat waves requires high quality historical climate data that offers good spatial and temporal distribution. To achieve this, rain gauges are installed to provide the most reliable measurement of rainfall. However, the rain gauge network is generally very poor in developing countries, leading to many uncertainties, especially in areas where no rain gauge is installed. To fill this gaps, rainfall estimation based on satellites seems to be a good and cost-effective alternative because they supply information for these areas at a relative low cost. However, these datasets are subject to systematic and random errors inherent to the observation method; therefore, there is a need to adjust them before their use for operational applications and decision making. This study proposes a rigorous method in three-step to improve satellite estimation data for Burkina Faso. The first step is devoted to assessing the accuracy of seven satellite precipitation datasets. Then the best dataset is bias corrected using Empirical Quantile Mapping (EQM) and Time and space-variant (TSV) bias-adjustment approaches. The final step is to generate blended datasets between the best corrected datasets and in-situ gauges data to produce more robust estimates of precipitation datasets. This blending was performed with Regression kriging (RK) and Mean Field Bias (MFB) with two interpolation techniques namely Shepard and Spheremap. The main results of the study are the following: The evaluation revealed that TAMSAT and CHIRPS were the best for daily and monthly time scales respectively. EQM method outperformed TSV at daily scale, while at the monthly scale the TSV was more suitable for bias correction. Morever, RK-Spheremap was the best of the four methods for merging satellite and in situ data at both time scales. Thus, the approach proposed in this study has improved the correlation coefficients improved the correlation of the daily data by 85.2% (from 0.147 to 0.999), the Bias by 12.4% (from 0.875 to 0.999) and the RMSE by 95.6% (from 26.494 to 1.175). Concerning the monthly dataset, the correlation coefficients are enhanced by 8.4% (from 0.916 to 1), the Bias by 2.3% (from 0.977 to 1) and the RMSE by 99.9% (from 35.654 to 0.042). This study may help in improving floods and droughts monotoring, as well as climate model validation over Burkina Faso.

Keywords: bias correction; datasets; merging; rain gauge; satellite; evaluation; statistical metrics.

Résumé

La gestion des risques climatiques tels que les sécheresses, les inondations et les vagues de chaleur nécessite des données climatiques historiques de haute qualité offrant une bonne répartition spatiale et temporelle. A cet effet, des pluviomètres sont installés afin de fournir la

mesure la plus fiable des précipitations. Cependant, le réseau de pluviomètres est généralement très pauvre dans les pays en développement, ce qui entraîne de nombreuses incertitudes, notamment dans les zones où aucun pluviomètre n'est installé. Pour remédier à ce problème, l'estimation des précipitations basée sur les satellites semble être une bonne alternative car ceux-ci fournissent des informations pour ces zones à un coût relativement faible. Toutefois ces données sont sujets à des erreurs systématiques et aléatoires inhérentes à la méthode d'observation; il est donc nécessaire de procéder à des ajustements avant leur utilisation pour des applications opérationnelles et la prise de décision. Cette étude propose une méthode rigoureuse en trois étapes pour améliorer les données d'estimation satellitaires pour le Burkina Faso. La première étape est consacrée à l'évaluation de la précision de sept ensembles de données de précipitations par satellite. Ensuite, les meilleurs jeux de données ont été corrigés des biais en utilisant les approches de correction des biais Empirical Quantile Mapping (EQM) et Time and space-variant (TSV). L' étape finale a consisté à générer des ensembles de données mixtes entre les données satellitaires corrigées de biais et des données in situ des pluviomètres afin de produire des estimations plus robustes des données sur les précipitations. Cette fusion a été réalisée avec les methodes Regression Kriging (RK) et Mean Field Bias (MFB) associés à deux techniques d'interpolation, à savoir Shepard et Spheremap. Les principaux résultats de l'étude sont les suivants: l'évaluation a révélé que TAMSAT et CHIRPS étaient respectivement les meilleurs pour les échelles de temps quotidiennes et mensuelles. La méthode EQM a surpassé TSV à l'échelle quotidienne, tandis qu'à l'échelle mensuelle, la TSV était plus adaptée à la correction des biais. En outre, RK-Spheremap a été la meilleure des quatre méthodes de fusion des données satellitaires et in situ aux deux échelles de temps. L'approche ainsi proposée dans cette étude a permis d'améliorer les coefficients de corrélation des données journalières de 85,2% (de 0,147 à 0,999), le biais de 12,4% (de 0,875 à 0,999) et le RMSE de 95,6% (de 26,494 à 1,175). À l'échelle de temps mensuelle, les coefficients de corrélation ont été améliorés de 8,4% (de 0,916 à 1), le biais de 2,3% (de 0,977 à 1) et l' EQM de 99,9% (de 35,654 à 0,042). Cette étude peut aider à améliorer le suivi des inondations et des sécheresses, ainsi que la validation des modèles climatiques au Burkina Faso.

Mots-clés : correction des biais; donnees; évaluation; pluviomètre; satellitaire; fusion; métriques statistiques.

Acronyms and Abbreviations

ANAM	:Agence Nationale de la Météorologie
ARC2	:Africa Rainfall Estimate Climatology version 2
CDO	:Climate Data Operator
ColCOK	:Co-located cokriging
CMORPH	:CPC MORPHing technique
CHIRPS	:Climate Hazards Group Infrared Precipitation
CPC	:Climate Prediction Center
CM	:Conditional Merging
CNSC	:Cadre national des Services Climatiques
CRU	:Climate Research Unit
DT	:Daily Transformation
ENACTS	:Enhancing National Climate Services
EQM	:Empirical Quantile Mapping
FAR	:False Alarm Ratio
GQM	:Gamma Quantile Mapping
GTS	:Global Telecommunications System
GHCN	:Global Historical Climate Network
GPCC	:Global Precipitation Climatology Centre
IDW	:Inverse Distance Weighted
IMERG	:Integrated Multi-satellitE Retrievals for GPM
IPCC	:Intergovernmental Panel on Climate Change
IR	:Infrared
IRI	:International Research Institute for Climate and Society
JAXA	:Japan Aerospace Exploration Agency
KED	:kriging with external Drift
LB	:Local bias
LOCI	:Local Intensity Scale
LS	:Linear Scaling
NASA	:National Aeronautics and Space Administration
NMS	:National Meteorological Services
NMHS	:National Meteorological and Hydrological Services
MAE	:Mean Absolute Error
ME	:Mean Error
MFB	:Men Field Bias

MSWEP :Multi-Source Weighted-Ensemble Precipitation
PANA :Programme d'Action National et d'Adaptation
PBIAS :Relative percent of bias
PERSIANN :Precipitation Estimation from Remotely Sensed Information
PREC/L :Precipitation reconstruction over land
PMW :Passive microwave
PNUD :Programme des Nations Unis Pour le Developpement
POD :Probability of Detection
FAR :False Alarm Ratio
SPD :Satellites based-precipitation estimates
RFE :African Rainfall Estimation
RMSE :Root Mean Square Error
RK :Regression Kriging
SOFF :Systematics Observations Financing Facility
SPD :Satellites precipitation data sets
TAMSAT :Tropical Applications of Meteorology using SATellite data)
SF :Spatial fixe
TARCAT :African Rainfall Climatology and Time- series
TRMM :Tropical Rainfall Measuring Mission
TSF :Time and Space Fixed
TSV :Time and Space-Variant
TSC :Temporal Spatial Constant
TV :Time variable
TIROS :Television InfraRed Observation
TIR :Thermal infrared
VIS :Visible
WMO :World Meteorological Organization

List of Tables

1.1 Summary of advantages, disadvantages, and intercomparison of bias corrections methods. 15
1.2 Summary of advantages, disadvantages, and intercomparison of Merging methods. 19

2.1 Summary of selected satellite rainfall datasets for this study 29

3.1 Statistical indicators for daily time scale 43
3.2 Statistical indicators for monthly time scale 46
3.3 Summary of daily bias correction statistical indicators 48
3.4 Summary of monthly bias correction statistical indicators 50
3.5 Summary of daily merging statistical indicators 52
3.6 Summary of monthly merging statistical indicators 55
3.7 Summary of enhancements to the TAMSAT daily dataset for Burkina Faso . . 58
3.8 Summary of enhancements to the CHIRPS monthly dataset for Burkina Faso . . 58
3.9 List of stations involved in this study, their coordinates and data availability on the study period (2001-2014) III

List of Figures

1 Frequent natural disaster and populations affected by those disasters from 1980 to 2020 in Burkina Faso. 2

1.1 Illustration showing the difference between passive versus active sensors. . . . 9
1.2 Meteorological satellite observation network 9
1.3 Electromagnetic Spectrum 11

2.1 Study area location within Africa and distribution of rain gauges used in this study 22
2.2 Precipitation anomaly time series plots of the three selected representative weather stations 24
2.3 Spatial distribution of rain gauges used in this study 25
2.4 overview of mean yearly precipitation of seven Satellite-based precipitation datasets and stations data from 2001 to 2014. 28
2.5 Flowchart of the Methodology 31
2.6 Schematic of the quantile mapping method. Adapted from Kim et al.(2016) . . 36

3.1 Taylor diagram for the three climatic zone obtained from spatial averaged of daily data 42
3.2 Taylor diagram for the three climatic zones obtained from spatial averaged of monthly values. 45
3.3 Comparison of monthly precipitation captured by satellites precipitation estimates datasets with rain gauge. 47
3.4 Taylor Diagram of daily data spatial average 49
3.5 Comparison of daily average rain gauge data with uncorrected TAMSAT and bias-adjusted TAMSAT datasets over the period 2001-2014. 49
3.6 Taylor Diagram of monthly data spatial average 51
3.7 Comparison of monthly average rain gauge data with uncorrected CHIRPS and bias-adjusted CHIRPS datasets over the period 2001-2014. 51
3.8 Taylor Diagram of daily data spatial average 53
3.9 Average of daily rain gauges data over 2001–2014, compared to TAMSAT unmerged data and TAMSAT merged 53
3.10 Comparison of daily rainfall (mm) for 29 july 2010 and 31 December 2010 between rain gauge, original TAMSAT and final data sets merged 54
3.11 Taylor Diagram of monthly data spatial average 56

3.12 Average monthly rain gauges data over 2001–2014, compared to CHIRPS unmerged data and CHIRPS merged 56
3.13 Comparison of monthly rainfall (mm) for September 2010 and December 2010 between rain gauge, original TAMSAT, and final data sets merged 57
3.14 Scatter plots of daily data between the rain gauge observations and the satellites precipitation datasets I
3.15 Scatter plots of monthly data between the rain gauge observations and the satellites precipitation datasets II

Introduction

Background and Context

Climate change has an impact on the environment, which changes the resources available to humans. Vulnerability to this phenomenon varies depending on geographic location, weather, and economic, social, and environmental conditions. The Sixth Assessment Report of IPCC cites Africa as the most vulnerable continent to climate change and variability (IPCC, 2022). The Sahelian zone of West Africa is particularly vulnerable to climate change, as the majority of its resources are climate-dependent, and the poverty of populations limits its access to suitable adaptation solutions (Roudier et al., 2011). Over the last four decades, severe changes in rainfall patterns have been documented, with reductions in rainfall from 36% to 50% (Ali and Lebel, 2008, Lebel et al., 2003). The decrease in rainfall during this period was characterized by severe droughts, which were considered the most significant global droughts of the twentieth century in terms of spatial and temporal extent, leaving catastrophic consequences that will be remembered for a long time. Moreover, in this region of Africa, climate crises are also characterized by floods due to heavy rains with serious consequences on the main socio-economic activities. Because of its geographical location in the Sudano-Sahelian zone of West Africa, Burkina Faso is not spared from the harmful effects of climate variability and change. Drought remains one of the most frequent and disaster in this country and it occurred during the last two decades of the 20th century, in 1973, 1984, 1991, 1994, 1998 and 2004 (PANA, 2003) due to low rainfall and uneven distribution. On the other hand, floods are also responsible for huge disruptions including loss of human lives and economic assets, as well as damage to infrastructure. Tazen et al.(2018) reported that they had increased in number and intensity in Ouagadougou and across the country, based on a review of historical flooding incidents.

Drought and floods have a negative impact on agriculture, the country's main economic sector, which accounts for 35% of GDP. The tragic flood of September 1, 2009, which affected more than 150,000 people and caused serious property losses and deaths, is still fresh in people's

minds. In addition, climate models and climate change scenarios predict a decrease in precipitation of 3.4% by 2025 and 7.3% by 2050 (PANA, 2007). The climate conditions described above reflect the high vulnerability to current and even future climatic shocks requiring adaptation measures to climate variability and change at local, national and global levels. Therefore, the provision of appropriate sector services could enhance adaptive capacity and resilience, thereby reducing the impact of extreme weather events. As a result, WMO created the National Framework for Climate Services (CNSC) intending to promote adaptation to climate change by producing and disseminating appropriate weather and climate data and services to different users and decision-makers. The priority sectors are agriculture, water resources, hydrometeorology, disaster warning, health and energy. In the same spirit, the World Meteorological Organization, in collaboration with a wide range of international organizations, created the Systematic Observations Funding Facility (SOFF) to help countries improve weather forecasts, early warning systems and climate information by providing technical and financial assistance to generate and exchange baseline observations. However, the effectiveness and reliability of all these actions fall within the framework of adaptation, such as climate forecasts, or any hydrological study, whether they are linked to flood forecasting, drought monitoring, management of water resources or the assessment of the impacts of climate change, depend heavily on the availability of good quality rainfall data. Good quality data includes a good spatial distribution across the country, but also a reasonable time series with as few missing data as possible. The figure 1 provides overview of the most frequent natural disaster and the impacts of those disasters on human populations from 1980 to 2020 in Burkina Faso.

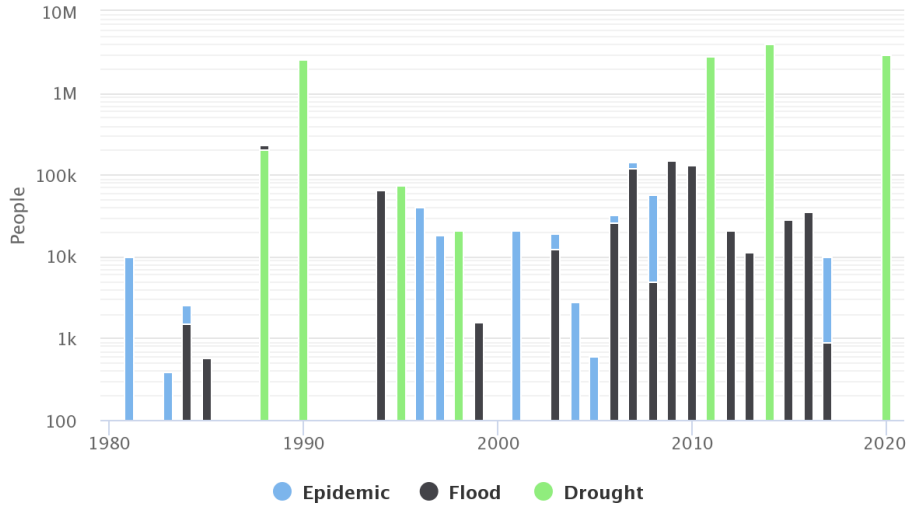

Figure 1: Frequent natural disaster and populations affected by those disasters from 1980 to 2020 in Burkina Faso.

Problem Statement

Precipitation data are usually provided from the National Meteorological Services (NMS) observation network. The suggested density of the ground-based precipitation network is 250 km^2 per station for mountainous regions and 575 km^2 per station for interior plains regions (WMO, 2008). However, the network of rain gauges in most of Africa is sparse, and long-term records are not always available (Dembélé and Swart, 2016). Various reasons explain this situation. Many of them are political, socio-economic and go far beyond the direct influence of NMHSs. They include civil wars, poverty, and more recently, regional epidemics. In Burkina Faso, as in other developing countries, the densification of a network of meteorological stations is not one of the government's priorities. The national meteorological services then lack the financial capacities and technical infrastructures to deal with the network of stations. Therefore least developed countries, such as Burkina Faso depend on international assistance to maintain their observation networks and related services (PNUD, 2016). Furthermore, in Burkina Faso, classified forests and protected areas cover an estimated 3.9 million hectares[1], or about 14% of the country's territory, making it impossible to establish a good network of stations. Weather radars seemed to be an alternative, but their exorbitant acquisition and maintenance costs limit the development of a radar network. Those in Ouagadougou and Bobo Dioulasso have not been in service for some years. In addition to this, insecurity has affected the management of the existing observation network, in that localities under terrorist threat have seen their populations empty, which implies the absence of observations by abandoning the stations.

Considering all these issues, acquiring a climatic record of precipitation amounts at a very fine spatial scale with a long time series over a given area has become a huge challenge. It makes managing extreme weather events and conducting scientific research difficult. To overcome the lack of measuring stations, satellite rainfall estimates are considered the best options for obtaining reliable rainfall data. These datasets are convenient due to their good temporal and spatial coverage and data sources in ungauged areas are also available (Katsanos et al.,2016). They provide data in inaccessible places such as forests, mountains, and dangerous areas. Satellites and radars, unlike rain gauges, estimate precipitation indirectly, hence their data is vulnerable to errors. The rain gauges have the advantage of high fidelity, while satellite estimates have good spatial and temporal coverage. It is therefore essential to take advantage of the strengths of both sources by merging the two datasets. This approach of combining satellite precipitation datasets with precipitation measurements would have a lot of benefits

[1]http://www.naturama.bf/web/index.php/component/k2/item/135-apercu-sur-les-aires-protegees-au-burkina-faso accessed 12-11-2021

(Duque-Gardeazábal et al., 2018). In this respect, some reflections have already been made by researchers to obtain reliable and high-resolution data by combining the precipitation datasets from the two sources. This is why, since the end of the 1990s, several blended datasets made up rain gauges, satellite and reanalysis are available. Among them, MSWEP and GPCP (Beck et al., 2017) have worldwide coverage, while IMERG, CHPclimv.1.0, and CHIRPS (Huffman et al., 2014) have regional coverage. In Africa, the Enhancing National Climate Services (ENACTS) approach, initiated by the International Research Institute for Climate and Society (IRI), has been implemented in eight countries at the national level. These countries are Mali, Ghana, Gambia, Ethiopia, Rwanda, Tanzania, Zambia, and Madagascar, where data from rain gauge networks has been blended with data from satellite rainfall estimates (Dinku et al., 2016) to improve the availability, quality and access to climate data. As can be seen, none of these studies have been carried out in Burkina Faso at the national level to produce a fine spatial resolution rainfall data with a long time series.

This study proposes a model to provide an improved rainfall Data set that can represent both a good temporal and spatial distribution for Burkina Faso. This will be done by blending satellite and rain gauge data in three procedures: (1) Assessing the performance of satellite precipitation datasets (2) bias adjustment of Satellites datasets , and (3) merging of datasets.

Outline of the thesis

This thesis is organized as following: An introduction including a general background related to the study topic, problem statement, objectives and hypothesis of this work. The relevance of the study is described in section as well. Chapter 1 presents the literature review in which precipitation observation systems are described as well as a depth review of the most common approaches for bias correction and datasets merging. Chapter 2 describes the methodology used to conduct the study. Then Chapter 3 presents and discusses the results of the study. Finally, a conclusion summarizes the main findings and contributions of the thesis. Possibilities for future research are also presented.

Research questions

Main research questions: How can the quality of gridded precipitation datasets in Burkina Faso be improved from rigorous scientific approaches? Specific research questions: The following

research questions must be answered to achieve the main objective:

- What are the performances of satellite precipitation datasets for each climatic zone in Burkina Faso at the daily and monthly time scales?
- What is the most effective rainfall bias correction algorithm for Burkina Faso?
- Do the satellite-gauges merging techniques employed improve the quality of the bias-corrected SPDs?

Research hypotheses

- As the evaluation time step increases, the performance of the SPDs improves.
- The bias-corrected dataset shows a significantly reduced systematic bias with EQM compared to TSV.
- The reliability of the bias-corrected datasets is improved by merging them with rain gauge observations.

Research objectives

This study aims to improve the quality of gridded precipitation datasets using rigorous approaches that combine satellite estimates and rainfall observations across Burkina Faso. This general objective is divided into three specific objectives which are:

- To evaluate the performance of seven satellite precipitation datasets by comparing them with rain gauge measurements at daily and monthly time scales for each climate zone.
- To investigate the effectiveness of two bias correction approaches in removing the systematic bias from the best daily and monthly datasets previously identified.
- To improve the reliability of the bias-corrected dataset (daily and monthly time scale) by blending the rain gauges and bias-corrected datasets using four merging algorithms.

Chapter 1

Literature review

1.1 Precipitation observation systems

Precipitation observation methods can be divided into two broad categories: direct measurement and indirect measurement. Direct measurements also called "situ" (in place) are carried out by rain gauges. In this type of measurement, the devices are in direct contact with the variable measured. On the other hand, indirect measurements, called remote sensing, consist of the estimation of precipitation by satellites and meteorological radars. Rain gauges and satellites will be discussed in detail below. For the radars which are not the subject of this study, a brief description will be given.

1.1.1 Rain gauge measurements

The rain gauge is historically the first instrument used to measure precipitation (Strangeways, 2010). It offers the advantage of simple and direct measurement, but the spatial representativeness of its measurement is very limited. The frequency of observations depends on the type of rain gauge used. Manual rain gauges are measured at long time intervals. Automatic tipping bucket rain gauges measure the accumulation time of a given water level on finer time scales (Sevruk, 1997). Thanks to the automation of the measurement and its transmission, the second type has the advantage of avoiding human intervention, which is always a source of errors. Rain gauge data is collected by the countries' national meteorological services. The World Meteorological Organization (WMO) promotes the densification of observation networks and ensures data concentration through the Global

Telecommunications System (GTS). To date, the total area of all operational rain gauges worldwide is surprisingly small, corresponding to 5.93 10^{-15}% of the earth's surface (Kidd et al., 2017). The global number of rain gauges is estimated at 250,000 by Groisman and Legates. (1995), while New et al., (2001) estimated their number at around 150,000. It is recognized that they are not evenly distributed over the globe, especially in parts of Africa, but also over the oceans, in desert areas. In situ measurements are only representative of a small area around the measurement site. One of the datasets composed of original rain gauge data is the Global Historical Climate Network (GHCN) [Menne et al., 2012] with daily and monthly temporal resolution. Due to the uneven distribution of observing stations, gridded data are increasingly needed. Several precipitation gridded datasets, entirely based on gauge information, have been constructed and are widely used (Kidd et al. 2017). The most common gauge-based datasets globally are CRU (Harris et al. 2014), GPCC (Becker et al., 2013), PREC/L (Chen and Xie, 2002), Udel (Matsuura and Willmott, 2009) and CPC-Global (Xie et al., 2010). The GPCC remains the most comprehensive and widely used rainfall database, covering the period from 1901 to the present day. In Burkina Faso, the rain gauge network consisted of nearly 134 observation stations including synoptic, climatological, agrometeorological and rainfall stations before 2016. Observations dating from 1902 exist for some stations. The network currently consists of nearly 260 automatic stations whose observations are very recent and therefore do not have long time series.

1.1.2 Uncertainties in rain gauge measurements

The measurement of rainfall by rain gauge is subject to an uncertainty mainly related to the measuring device (the rain gauge) on the one hand and to its environment on the other hand. Indeed, the natural and/or human surrounding conditions (vegetation, buildings, insect intrusion, etc.) are sources of error. This is why the choice of the location of a rain gauge is crucial to guarantee a good measurement of precipitation: a device located near a building will underestimate the precipitation according to the wind direction (on the ground). Moreover, changing the measuring equipment or moving it to another observation site may alter the continuity of the precipitation observation series. It is therefore important to carry out quality control of the precipitation observations before climatological studies. Although the measurement of precipitation by rain gauges generates uncertainties, when it comes to assessing the performance of models, ground-based rain gauges are always considered as reference data and therefore as correct data.

1.1.3 Meteorological Radars

Radar stands for radio detection and ranging and is a system that uses microwave energy for the detection and ranging of objects. Weather radars can generally be divided into fixed position radars and mobile radars. The latter are either transported in a vehicle or transported on board an aircraft or a satellite. The radar is an active system that emits by itself electromagnetic waves in a direction of space and captures the wave reflected by a target (hydrometeor). The mechanical scanning of the system allows complete coverage of the space surrounding the radar. Depending on the power emitted and the wavelength used, the range of the radar varies from a few kilometers to 500 km, but in general, its useful range is limited to less than 300 km [1]. Nowadays, conventional radars are replaced by radars capable of detecting not only the intensity of precipitation but also its speed of movement (Doppler effect). To cover very large areas, several radars can be used in a network.

1.1.4 Satellite precipitation estimates

Remote sensing is the science of acquiring information about an object or phenomenon without coming into physical contact with the object, unlike in situ or on-site observation. In current usage, the term generally refers to the use of satellite or aircraft-based sensor technologies to detect and classify objects on Earth, including on the surface and in the atmosphere and oceans, based on propagated signals (e.g., electromagnetic radiation). Then, electromagnetic radiation is indirectly converted to precipitation rate by algorithms. Since the 1960s when the first Television and IR Observation Satellite (TIROS) was launched, the number of remote sensing satellites for Meteorology purposes keeps growing. It has increased by 73% in 2017 from the update of 2016 (Lavender, 2017)[2]. Figure 1.2 shows the global network of operational meteorological satellites in 2011. Two types of sensors are commonly used in satellite rainfall-estimation algorithms, the active sensors from geostationary satellites and the passive sensors on polar-orbiting satellites (Figure 1.1).

- Passive RS (i.e., when the reflection of sunlight is detected by the sensor), the only source is the sun (day-light conditions).
- Active RS (i.e., when a signal is emitted by a satellite or an aircraft themselves and its reflection by the object is detected by the sensor; sensor supplies its power source),

[1] https://www.radartutorial.eu/druck/Chapitre2A.pdf accessed 03-03-2022
[2] https://www.pixalytics.com/eo-sats-in-space-2017/

imaging is independent of daytime or nighttime conditions.

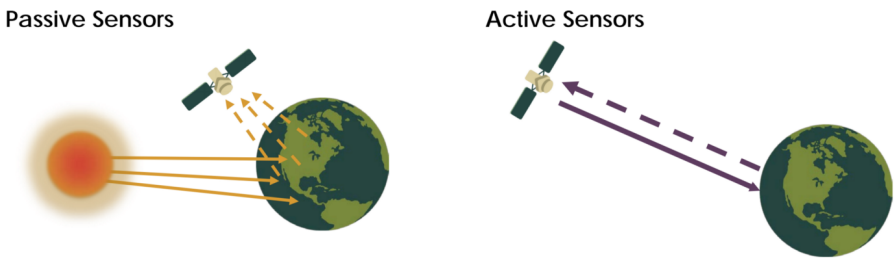

Figure 1.1: Illustration showing the difference between passive versus active sensors.

Source:[3]

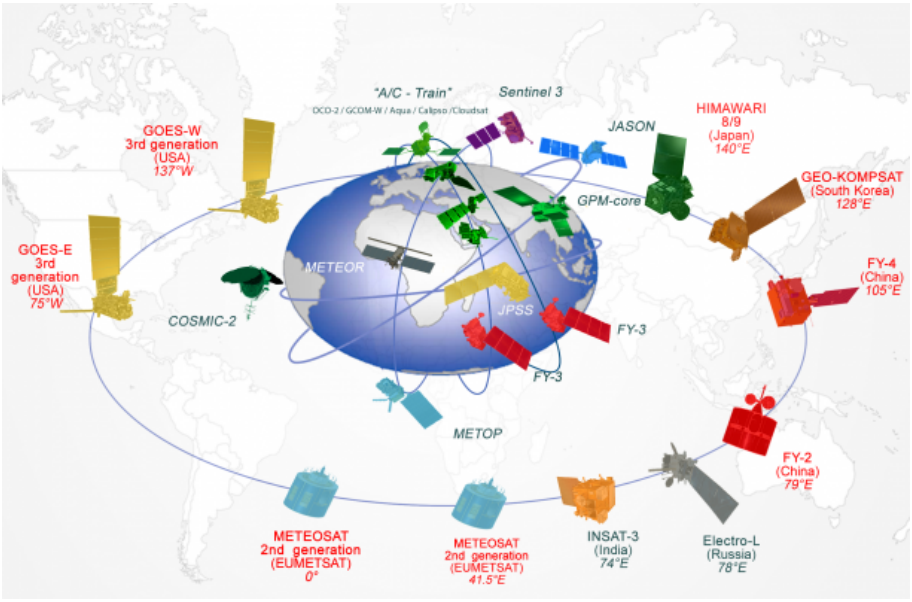

Figure 1.2: Meteorological satellite observation network

Source: WMO[4]

1.1.4.1 Satellite measurement principles

The methods used onboard meteorological satellites for precipitation observations are mainly visible (VIS) / infrared (IR), Passive microwave (PMW) systems (Nicholson et al., 2003),

[3]https://public.wmo.int/en/programmes/wmo-space-programme accessed 22-03-2022
[4]https://earthdata.nasa.gov/learn/remote-sensors accessed 22-03-2022

and the Multi-Sensor Technique. Today, dozens of Earth observation satellites are in orbit, constantly providing thousands of images for military applications, but also increasingly for civilian applications.

The Visible and Infrared

The Thermal infrared (TIR) sensors from geostationary satellites. The VIS and IR domains have wavelengths between [0.4; 0.75] and [0.75; 1000] respectively (figure 1.3). The observation of precipitation in both spectra is related to the characteristics of cloud tops (Lensky and Levizzani, 2008). In the visible range, with solar radiation, clouds reflect strongly and appear brighter than land surfaces, so the brightness depends on the vertical extension of the cloud. For this reason, VIS channels can also be used to determine the type of cloud. Rough cloud tops are characteristic of clouds with strong lift, while smooth cloud tops define stratus clouds. This method is exclusively dependent on solar radiation. IR estimates precipitation by measuring temperatures at the cloud top. In contrast to the visible, this technique works at night. The principle is based on the fact that the colder the cloud top is, the more it will develop vertically and therefore generate higher precipitation rates. The advantages of IR are the high temporal sampling (every 15 minutes), the fine spatial resolution (<3km), and the wide coverage when used from geostationary satellites. However, this relationship between cloud top temperature and precipitation rate is an indirect relationship that varies with rainfall systems. The VIS and IR methods have drawbacks in that they measure cloud-top properties instead of rain at the ground (Capacci and Porcu, 2009). The rainfall estimation method is not therefore physical. In the case of cirrus clouds, which are made of ice crystals and therefore very cold, will be considered precipitating clouds, while this kind of cloud does not generate rain.

Passive Microwave

Passive microwave sensors (PMW) are carried on satellites in polar orbit. The microwave part of the spectrum covers a range of wavelengths from 1 centimeter to 1 meter (Figure 1.3). These wavelengths are long compared to visible and infrared waves, so microwaves have special properties in remote sensing. The longer waves pass through cloud cover, drizzle, dust and light rain because they are not susceptible to atmospheric scattering which affects the shorter waves. Clouds and precipitation emit, absorb and scatter radiation. Microwave sensors measure the brightness temperature from the top of the atmosphere to the satellite. This property allows detection in almost all atmospheric conditions, and therefore data acquisition at any time. MW techniques are therefore physically more direct than those based on VIS/IR radiation. However, microwave sensors have a poor spatial and temporal resolution (Levizzani et al., 2001). The

brightness temperature is calculated by inverting the Planck function as shown in equation(1).

Formula		**Explanation**
$T_B = B_\lambda^{-1}(I_\lambda) = \frac{C_2}{\lambda \ln[(\frac{C_1}{\lambda^5 I_\lambda}) + 1]}$	(2.1)	**Bλ** is the planck function **Iλ** is radiance c_1 = 1.191044 x 10-5 (W/m²) c_2 = 1.438769 (cm deg K)

Multi-Sensor Technique

Multi-source satellite estimates result from the merging of infrared and microwave data from different operational satellites. The combination of VIS/IR and PMW is an opportunity to combine good sampling (VIS/IR) with better extractions (PMW) to not only improve estimates but also spatial and temporal resolution (Ringard, 2017). Passive microwaves have the advantage of capturing precipitation well and, for IR, following the distribution of precipitation. To this end, several algorithms have been developed to combine PMW and IR (Joyce et al., 2004).

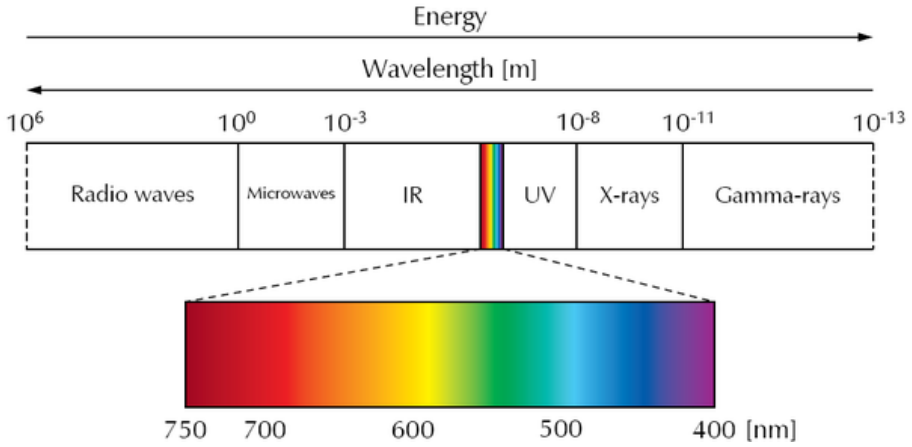

Figure 1.3: Electromagnetic Spectrum

Source:[5]

[5]https://www.japanistry.com/electromagnetic-spectrum/ accessed 22-03-2022

1.2 Evaluation of SPDs

1.2.1 Summary of the previous studies on the evaluations of SPDs

The reliability of SPD datasets in reproducing ground-based precipitation needs to be assessed (Meng et al., 2014) due to uncertainties in these datasets. With regard to the evaluation of satellite data, data from rain gauges are still used as a reference to evaluate the ability of satellite data estimation algorithms to reproduce precipitation on the ground. Numerous studies have examined the performance of SPDs in several regions of the world. In China (Jiang et al., 2019), in the islands (Katsanos et al., 2016), in Iran (Javanmard et al., 2010), in the Pacific Ocean (Pfeifroth et al., 2013), in Italy (Conti et al., 2013). Similar researches have been conducted in Africa, such as in the southern part (Toté et al., 2015), the eastern part (Bayissa et al., 2017), the west and the Sahel (Dembélé and Zwart, 2016, Atiah et al., 2020). This work covers different timescales, including daily, monthly, seasonal and annual (Dembélé and swart, 2016; Atiah et al., 2020).

1.2.2 Verification statistics for precipitation satellite datasets

There are well-known methods and statistics in the literature to assess the ability of SPDs to detect the occurrence and amount of precipitation. Continuous verification statistics measure the accuracy of a continuous variable such as the amount or intensity of the precipitation. The most commonly used continuous verification statistics are Pearson's correlation coefficient (r), mean error (ME), root mean square error (RMSE) and bias, mean absolute error (MAE) and percentage relative bias (PBIAS). Categorical verification statistics are used to measure the correspondence between the estimated and observed occurrences of events (Ebert, 2007) like Probability of Detection (POD) and False Alarm Rate (FAR) (Qin et al., 2014).

1.2.3 Some verification results of precipitation satellite datasets

Research results reveal that SPD performance differs between geographies and seasons for the same type of data (Gebremichael et al., 2014). This indicates that the performance of satellite datasets is highly dependent on the location, topography, season, and hydro-climatic characteristics of the study area. For example, Dinku et al. (2010) have shown that SPDs perform poorly in dry areas and mountainous terrain. The CHIRPS satellite dataset fared better in low-lying locations, according to Shrestha et al. (2017). The four satellite precipitation data

sets (TRMM-3B42, TRMM-3B42RT, CMORPH, GSMaP) performed better in summer than in winter. They also performed better in wet southern regions than in dry northern or high altitude regions, as argued by Qin et al. (2014). In addition, the reliability of satellite rainfall estimates varies with time scale. Evaluating TRMM-3B42 v7 in Morocco, Tramblay et al. (2016) found that the satellite estimates perfectly reproduced observed precipitation at monthly and annual time scales, but were less efficient in detecting extreme precipitation in Nepal. Gosset et al. (2013) assessed the accuracy of CMORPH and concluded that it overestimates daily rainfall in Niger by an average of 2 mm. CMORPH has also shown poor performances in West Africa and Ethiopia (Jobar et al., 2011; Dinku et al., 2008). Very few studies have been conducted in Burkina Faso. Dembélé and swart. (2016) evaluated the skill of SPDs (ARC2, CHIRPS, PERSIANN, RFE, TAMSAT, and TRMM) with the 10 synoptic weather stations in Burkina Faso. CHIRPS was found to be the best performing, while TAMSAT was found to be the worst. In numerous research, CHIRPS was also among best-performing datasets (Beck et al., 2017, Toté et al., 2015, Bayissa et al., 2017, Atiah et al., 2020)

1.3 Bias Correction of SPDs

1.3.1 Satellites -Rain Gauge Bias Correction Methods

Satellite Estimates are subject to different types of errors which errors arise from two sources: (1) random error, which is inherent in measurement records (Tang et al., 2015), and (2) systematic bias related to post-processing algorithms and procedures (Sadeghi et al., 2019). As described in Smith et al., (2006), this systematic difference between satellite and terrestrial observations is known as bias. Thus, they must be adjusted before being used as input data for hydrological models or other applications (Gumindoga et al., 2019). Several “bias correction” techniques have been developed in an attempt to improve SPDs and are discussed in detail in numerous publications (Themeßl et al., 2011; Teutschbein and Seibert, 2012; Lafon et al., 2013; Chen et al., 2013). Table 1.1 presents eight widely used methods. They can be classified into two main categories: dynamic bias correction methods also called Spatio-temporal bias correction methods such as Time and Space Variant (TSV), Fixed Time and Space (TSF), and Time variable (TV). The other category concerns the statistical methods of correction which can also be subdivided into linear methods, Nonlinear methods, and distribution-based methods as described in table 1.1.

1.3.2 Relative Advantages and Disadvantages of the most common Correction Methods

Each of the bias correction approaches analysed individually has strengths and weaknesses. Table 1.1 summarises the results of previous studies on the advantages and disadvantages of the methods discussed in the previous section (1.3.1). From this table it can be seen that the linear adjustment methods are able to adjust the mean (LS) as well as the frequencies and intensities of the rainy days of the rainfall time series (LOCI). They are limited because they do not take into account changes in the frequency distribution of rainfall. Non-linear (NL) and distribution-based methods correct the mean as well as the variance of the estimated rainfall time series. Dynamic methods have the advantage of correcting for both spatial and temporal aspects of the bias.

1.3.3 Intercomparison of bias Adjustment Methods

Researchers are still working on evaluating different bias correction methods and, to date, the literature does not provide any references regarding the best bias correction technique (Goshine, 2020). Table 1.1 summarises the results of comparative studies of bias correction methods. Not all methods generally improve all statistics and methods are often compared according to the indicator targeted or to be improved. In general, linear methods can be considered the least effective as they are designed to change only the mean and ignore any lack of correction for rainfall occurrence. It is reported that the distribution-based approach has been more successful in reproducing precipitation than both linear and non-linear approaches. Empirical quantile mapping remains the most widely used bias correction and is also known to be the most effective. Among the dynamic methods, TSV performed better than TSF and TV in the majority of evaluation studies. Overall, when comparing EQM and other bias correction methods, EQM is superior.

Table 1.1: Summary of advantages, disadvantages, and intercomparison of bias corrections methods.

Statistical Bias correction Methods				
Bias corr Methods	Advantages	Disavantages	Intercomparaison	references
1. Linear scaling (LS) (Linear Methods)	- Simplest bias-adjusted method - adjust perfectly the climate factors when the monthly average values are included.	– It does not correct the standard deviation or variance and all events are adjusted with the same correction factor - the number of the wet day is larger than observed wet day	- the linear method showed the weakest correction because it is designed to modify only the mean.	(Teutschbein and Seibert 2012; Lenderink et al., 2007; Lafon et al., 2013)
2.Local intensity scaling (LOCI) (Linear Methods)	- overcomes the limits of LS - corrects wet-day frequency and wet-day intensity.	- It does not capture the different changes in the frequency distribution of precipitation. - No adjustment is made to the of daily precipitation occurrence.	- the linear method showed the weakest correction because it is designed to modify only the mean	(Schmidli et al., 2006)
3.Power transformation (PT) (Non-linear Method	- Corrects mean and standard deviation (variance) of the precipitation series - events are adjusted non-linearly	- No adjustment is made to the temporal structure of daily precipitation occurrence. - adjusts wet-day frequencies and intensities only to some extend (d*)	- nonlinear BC schemes (power transformation) were most effective in reproducing rainfall totals. - The PT scheme was found to be the best	(Leander and Buishand 2007; Gumindoga et al., 2016; Soo et al., 2020)
4.Empirical Quantile mapping (EQM) (Distribution based Method)	- corrects mean, standard deviation (variance), wet-day frequencies and intensities - The cumulative distribution function does not need prior definition. - it corrects quantiles and preserves the extreme rainfall values	- the effectiveness of the QM is influenced by the sample size that is used to calculate PDFs. When the sample size is insufficient, the uncertainty enlarges, and vise verse. - It may not capture the the temporal structure of daily precipitation occurrence.	- Quantile mapping shows the best performance, particularly at high quantiles. - Distribution mapping performs the best for both climate projections and hydrological impact qualifications	(Themeßl et al., 2012; Alharbi 2019); Themeßl et al., 2011; (Teutschbein and Seibert 2012; Lenderink et al., 2007)
5.Gamma Quantile mapping (GQM) (Distribution based Method)	- corrects mean, standard deviation (variance), wet-day frequencies and intensities - The occurrence of precipitations is corrected by Local Intensity Scaling method	- This accuracy is valid only when the observed and modelled precipitation data are -distributed - No adjustment is made to the temporal structure of daily precipitation occurrence.(a*)	- offers the best combination of accuracy and robustness - The distribution-based methods are consistently better than the mean-based methods for both precipitation projections and hydrological simulations	(goshime, 2020; Omondi, 2017; Lakew et al., 2020)

Dynamic or Spatio-temporal Bias correction methods				
Bias Corr Methods	Advantages	Disavantages	Intercomparaison	references
6. Time and space fixed (TSF)	- advantages due to its ease of implementation, which requires less data entry - more effective in correcting the mean values of the satellite rainfall.	- deterioration of the monthly agreement probably since their temporal variation is too pronounced to be ignored. - can't fully correct the systematic error in rainfall frequency, especially during wet day values	- The TSF and TSV manifest poor performance even from the uncorrected WaterGAP3 products. - TSF correction shows low change than TSV correction	(goshime, 2020; Omondi, 2017; Lakew et al., 2020)
7. Time variable (TV)	- advantages due to its ease of implementation, which requires less data entry	- can't fully correct the systematic error in rainfall frequency especially during wet day values	- The TSC and SV manifest poor performance even from the uncorrected WaterGAP3 products	- (goshime, 2020; Omondi, 2017; Lakew et al., 2020)
8. Time and space-variant (TSV)	- advantages due to its ease of implementation, which requires less data entry - apply correction over time and space depending on the variability of rainfall estimate - removes all the cumulative rainfall differences in the data set.	- can't fully correct the systematic error in rainfall frequency especially during wet day values	- superior robustness of the TSV correction - TSV manifests significant the improvement compared to the other schemes - TSV outperforming DT and the rest of the bias schemes - TSV correction shows noticeable change than TSF correction.	(Habib et al., 2014; Stisen et al., 2012 ; goshime, 2020; Omondi, 2017; Lakew et al., 2020)

1.4 Merging of SPDs and rain gauges data

1.4.1 Satellites -Rain Gauge Blending Methods

Previous studies have shown that the approach of combining satellite precipitation datasets with precipitation measurements would have many advantages (Duque-Gardeazábal et al., 2018, Bhuiyan et al., 2019). In this regard, there have already been reflections by researchers to obtain reliable and high resolution data by combining the two sources of precipitation data. Thus, since the late 1990s, several mixed datasets (rain gauge and satellite, reanalysis) are available. Table 1.2 shows eight data merging methods, some of which are very recent. The merging methods can be classified as: adjustment methods; rain gauge interpolation methods using the spatial association of satellites as additional information (e.g. KED and ordinary kriging) and satellite-rain gauge integration methods (e.g. Bayesian and CoK). However, bias adjustment and interpolation methods are widely used and tested than integration methods (Ochoa-Rodriguez et al., 2019, Qiu et al 2020).

1.4.2 Relative Advantages and Disadvantages of some blending Methods

Table 1.2 shows some of the methods commonly used to merge data between satellites and rain gauges or between radar and rain gauges. It also indicates the advantages and disadvantages of using these methods. Merging methods have relative strengths and weaknesses, which may make them more or less suitable for a given domain (since domains have different physical characteristics). Methods that seem easier to implement quickly, for example, kriging with external drift (KED) and mean field bias. Others give a good visual impression of precipitation map estimates in sparse area gauges, such as co-located cokriging (ColCOK) and the dual kernel smoothing algorithm. On the other hand, some require a fairly dense network of rain gauges, such as ordinary kriging. Others are more suitable for small domains, such as the K-nearest neighbor local polynomial. Some cannot be applied to very fine time scales (e.g. daily) in which case the Bayesian approach or gives very high biases at these time scales (Kriging with External Drift (KED)). The most difficult to achieve is regression kriging as it is a mixture of two methods.

1.4.3 Intercomparison of Merging Methods

Table 1.2 summarises the results comparing merging methods. The methods belonging to the bias adjustment category, generally show the lowest performance. They are outperformed by the interpolation category or integration category such as regression kriging and Bayesian.

Table 1.2: Summary of advantages, disadvantages, and intercomparison of Merging methods.

Dynamic methods or Spatio-temporal methods Bias correction				
Blending Methods	Advantages	Disavantages	Intercomparaison	references
1. Ordinary kriging (OK) (Interpolation category)	- useful in regions with a well-distributed network of gauges	- no changes in data-sparse regions compared to raw SPDs - usefulness in sparse gauges regions - Assumes daily rainfall is continuous in space - prones to larger errors at smaller time steps	- (OK) has the lowest performance than RK.	(Chappell et al 2013, Verdin et al 2016; McKee, 2015; Hengl et al., 2007 , Pham et al., 2019)
2.Kriging with external drift (KED) (Interpolation category)	- The KED technique seems to be computationally more straightforward	- prones to larger errors at smaller time steps due to the presence of these fluctuations.	-KED was determined to provide the best representation - KED and Bayesian have similar performances which are superior to MFB	- (Hengl et al., 2007; Goudenhoofdt and Delobbe 2009; Ochoa-Rodriguez et al., 2015)
3. Regression kriging (RK) (Interpolation category)	- regression kriging is a mixed interpolation technique - no danger of instability like KED - the ability to extend the method to a broader range of regression techniques and to allow separate interpretation of the two interpolated components.	- it is more complex technique and, if misused, can give even worse estimates than straightforward ordinary kriging - RK requires a large number of sample points to fit the regression model. - prone to larger errors at smaller time steps due to the presence of these fluctuations.	- RK model was superior over OK, SK, MLR and IDW - RK was supereior over OK, KED and COK. - (RK) has a higher performance than OK.	(Goovaerts, 1997; ; Goovaerts, 1999; Hengl et al., 2004 and Sumfleth et al., 2008; Simbahan et al., 2006; Hengl et al., 2007, Pham et al., 2019)
4.Double-kernel smoothing algorithm (Interpolation category)	- shows good visual performance in a sparse stations area - error does not increase significantly when the rain gauge network density is reduced	–	- DS delivered the most consistent improvement over the satellite data set followed by the MBC method	- (Duque-Gardeazábal et al., 2018; Nerini et al., 2015)
5. Mean Field Bias (Bias adjustment category)	- The simplest and fastest these methods - smoothens the fluctuations that can be identified in individual gauges	- -	- LB and CM are better methods than MFB. - MFB correction method provided the greatest.	- (Giarno et al., 2020, Qiu et al., 2020; McKee, 2015; Giarno et al., 2018)

Dynamic methods or Spatio-temporal methods Bias correction				
Blending Methods	Advantages	Disavantages	Intercomparaison	references
6. Bayesian approach (Integration category)	- it has a good ability to represent wet events.	- invalid at finer temporal scales (i.e.,daily) due to the Gaussian assumption - its Gaussian assumption can result in negative estimates of precipitation in very dry regions	Bayesian approach outperforms MFB	- (Verdin et al., 2016; Wang et al., 2013)
7. Collocated cokriging (Integration category)	- improves the visual impression of the rainfall map estimates - minimizes the variance of estimation by solving a simple kriging system.	- overestimate daily rainfall only slightly	- ColCOK technique, provides good agreement compared with BK gauges and TRMM alone.	- (Teng et al., 2017)
8.Co-kriging (COK) (Interpolation category)	-Improves estimates using related secondary information	- blended estimate has a spatial structure very similar to the satellite-derived estimates.	- The LP model captures the spatial variability very well than Co-kriging.	(Verdin, 2013)

1.5 Summary of gaps based on literature review

Based on this review, in Africa, the Enhancing National Climate Services (ENACTS) approach, has been implemented in eight countries at the national level. These countries are Mali, Ghana, Gambia, Ethiopia, Rwanda, Tanzania, Zambia, and Madagascar, where data from the stations' network were combined with data from satellite rainfall estimates (Dinku et al ., 2016). All then benefited from improved availability, quality, and access to climate data. As can be seen, none of these studies have been carried out in Burkina Faso at the national level to produce fine spatial resolution rainfall data with a long time series. Thus, it is necessary to provide improved rainfall Data sets that can represent both a good temporal and spatial distribution for Burkina Faso. Unlike merging satellites and gauges directly like in many studies this study proposes steps before Merging: (1) an evaluation of SPDs, (2) bias correction. Going through steps (1) and (2) aims to reduce the systematic error before the merging step (3). The choice of Methods to conduct steps (1), (2), and (3) is discussed in section III.4 and takes into consideration the review above to significantly minimize the bias.

Chapter 2

Methodology

2.1 Study Area

2.1.1 Geographic location

Burkina Faso is a country in the center of West Africa, which covers an area of 274,000km^2, a landlocked country in the heart of West Africa. It is located between 9°20 and 15°05 North latitude, 5°30 West longitude and 2°20 East longitude and shares these borders with six other countries (Mali, Niger, Ivory Coast, Ghana, Togo, Benin). see figure 2.1.

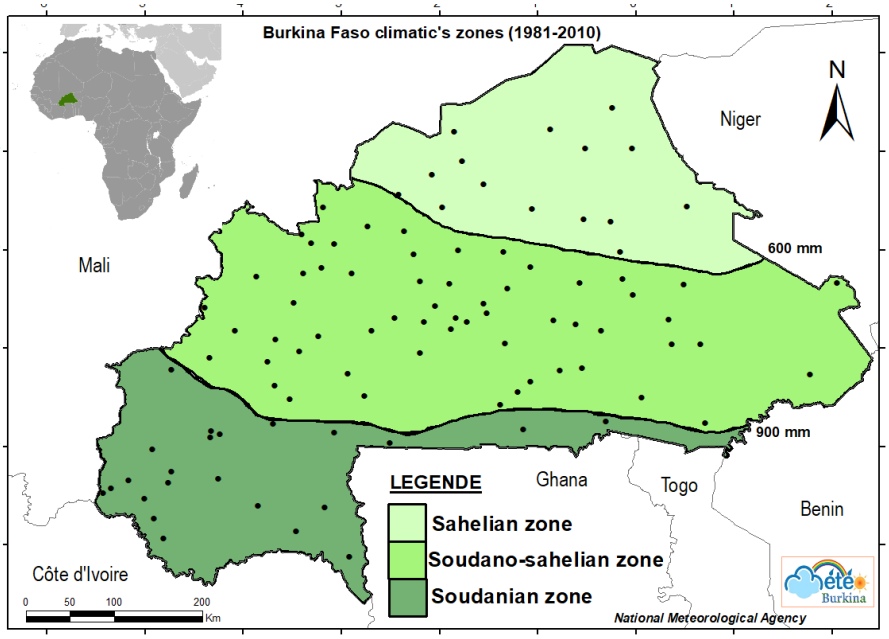

Figure 2.1: Study area location within Africa and distribution of rain gauges used in this study

2.1.2 Climatology

The rainfall regime of the Sahelian climate is characterised by the alternation of a short rainy season and a long dry season. This seasonal rhythm depends on the Saharan winds and the oceanic monsoons that circulate from the Saharan high pressure to St. Helena High. In the dry season, the continental trade wind, a hot and dry wind also called Harmattan, blows over the whole of Burkina Faso from October to March in a north-easterly direction. From March onwards, the overheated Sahara becomes a low-pressure area that sucks in oceanic air masses. The Harmattan is then replaced by the Boreal Trade Wind, a humid air flow blowing in a south-westerly direction. The position of the two annual rainfall isohyets (600mm and 900mm) makes it possible to define the three climatic zones as shown in Figure 2.1. Thus, the country can be divided into three main climatic zones which are:

- The Sahelian zone in the north is characterized by an annual rainfall of less than 600mm. The rainy season (with an average rainfall of less than 600mm/year). The rainy season begins in the Sahelian zone in June or early July and ends in September. The average number of rainy days is 110.
- The Sudano-Sahelian zone in the center is characterized by an annual rainfall of between 600 and 900 mm; the rainy season begins between May and June with an average number of rainy days equal to 150 days.
- The southern Sudanian zone where annual rainfall is between 900 and 1200 mm. The rainy season starts slowly from the end of March to the beginning of April in this zone with an average number of rainy days between 180 and 200 days (PANA, 2007).

Rainfall is abundant during the July-August-September quarter when more than 60% of the annual total is recorded.

Figure 2.2 shows the anomaly time series plots of the three selected representative weather stations (i.e. Dori, Ouagadougou and Bobo Dioulasso) located in the Sahelian, Sudano-Sahelian and Sudanian zones respectively, for the period 1981 to 2021. They show the high interannual variability of rainfall and the severe droughts that occurred in the Sahelian regions during the 1970s and 1980s. Negative anomalies are much more observed in Dori and Ouagadougou, reflecting the high vulnerability of the Sahelian zone compared to the more southern regions.

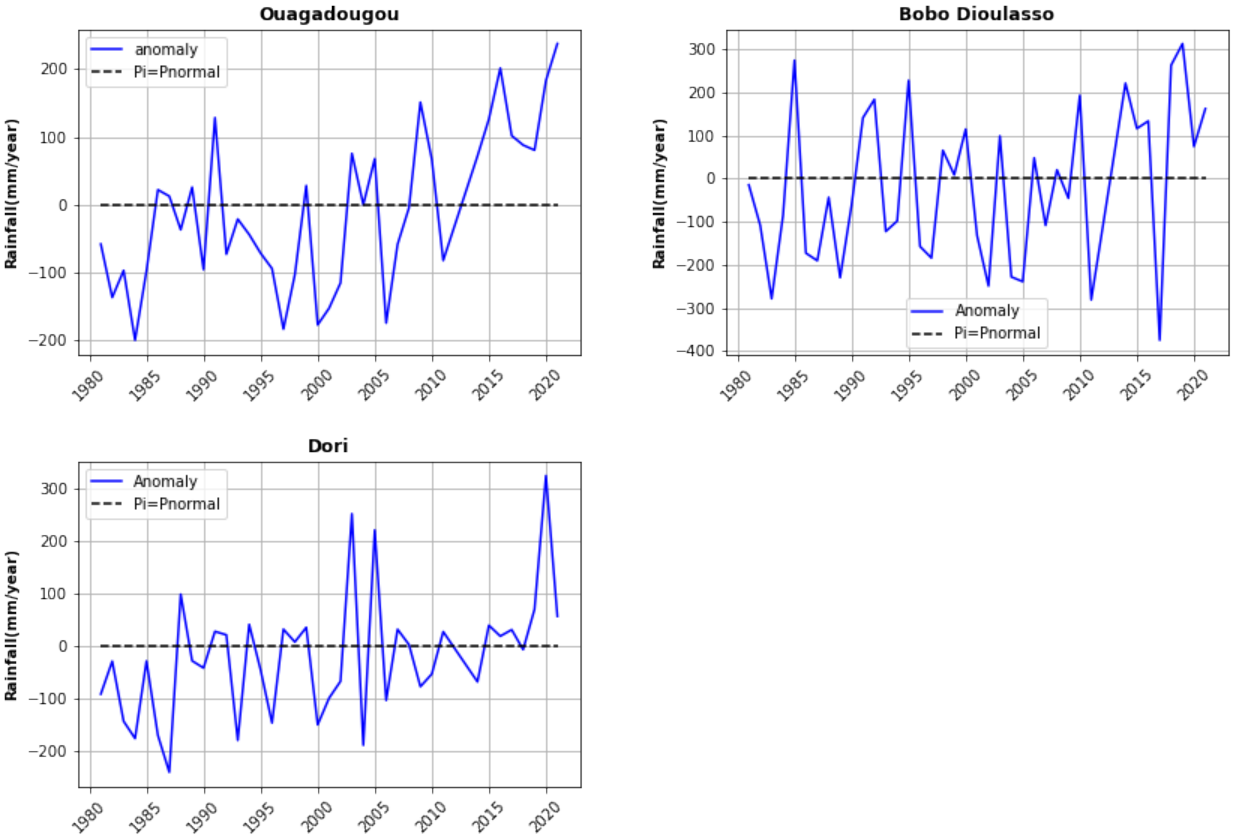

Figure 2.2: Precipitation anomaly time series plots of the three selected representative weather stations

2.2 Data

2.2.1 Rain Gauges data

The rainfall data used in this study were provided by the National Meteorological Agency of Burkina Faso (ANAM), Climatology Service. These data come from synoptic stations, Agrometeo stations and climatological stations and rainfall stations observed over the period from 2001 to 2014. Although the number of stations is relatively good, their distribution over the territory is not uniform. A summary of these ground measurements, the name of the station, its longitude and its latitude are given in appendix 3. The quality control of rainfall data from each station consists of checking the coordinates and identifying missing values. Stations with large data gaps between the selected validation period were excluded from the analysis. Only those with at least 95% of daily data available were retained for the study, i.e. 4857 out of 5113 days of data. Thus, of the 134 stations received from the National Meteorological Agency, only

97 stations were found to be reliable and compliant with the above criteria. The distribution of these stations over the climate zones is shown in Figure 2.3 as follows : 15 stations in the Sahelian zone; 59 stations in the Sudano-Sahelian zone and 25 stations in the Sudanian zone.

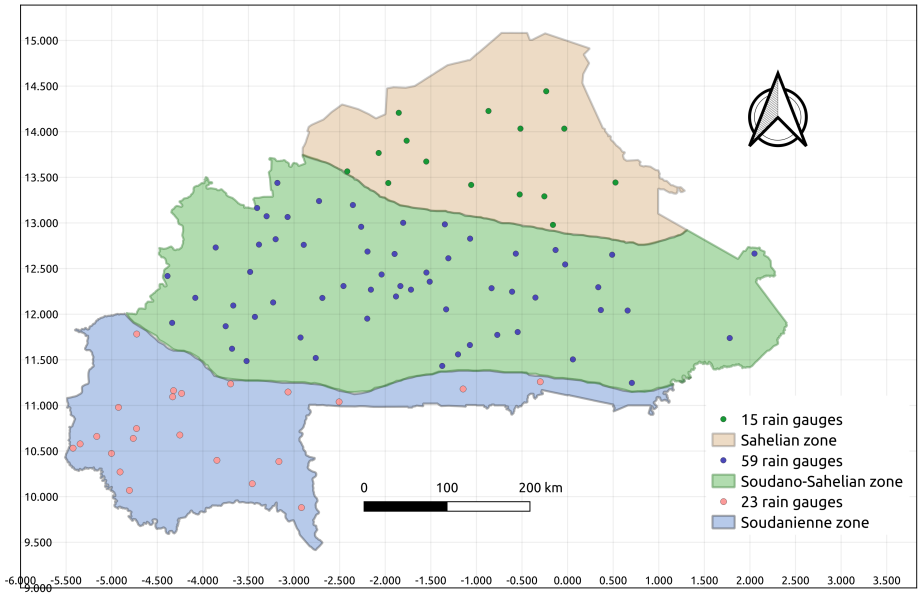

Figure 2.3: Spatial distribution of rain gauges used in this study

2.2.2 Satellite Precipitation datasets

Validation and inter-comparison of seven satellite rainfall datasets were carried out at daily and monthly scales. The satellite data are available on the Internet and were downloaded from the servers of the data producing institutions. Table 2.1 below gives more details on these different data sets. The seven satellite datasets selected for validation have spatial resolutions ranging from 0.04° to 0.5°. The choice was made based on the length of the series and also on the results of previous studies showing the reliability of these datasets. The motivation for the study period (2001-2014) is based on the wish to have a large number of satellite datasets to compare since they do not have the same start date. ARC2 and RFE had 8 and 1 days of missing data respectively over the study period. A summary of the satellite rainfall datasets used in this study is presented in Table 2.1. They are : CHIRPS V2; ARCv2; RFEv2; PERSIANN-CDR; TRMM -3B42V7; GPCP V3.1; TAMSAT V3.1).

- The CHIRPS datasets, developed by the US Geological Survey (USGS) and the Climate Hazards Group at the University of California are blended products which combine

global climatologies, satellite observations and in-situ rainfall observations from Global Telecommunications system (GTS). CHIRPS incorporates 0.05 of resolution starting in 1981 to near-present.

- ARCv2 is produced by the National Oceanographic and Atmospheric Administration Climate Prediction Center (NOAA-CPC) and provides daily rainfall data over Africa. It is very similar to RFEv2 except the 30 minutes is replaced by the 3-hourly IR data. The RFEv2 is also provided by NOAA-CPC for Famine Early Warning Systems Network to assist in disaster-monitoring activities over Africa.

- RFEv2 is also provided by NOAA-CPC for Famine Early Warning Systems Network to assist in disaster-monitoring activities over Africa. RFEv2 has been operational since 2001 and uses rainfall estimates from PM sensors, IR data from METEOSAT and daily rainfall from the GTS reports. Daily rainfall estimates were obtained at 0.1 of spatial resolution by merging these sources.

- PERSIANN-CDR (Precipitation Estimation from Remotely Sensed Information using Artificial Neural Networks - Climate Data Record) were developed by the Center for Hydrometeorology and remote sensing at the University of California (Ashouri et al., 2015). It uses an artificial neural network approach to merging the IR and PM data and the rainfall estimates are based on the infrared brightness temperature image provided by geostationary satellites (Hsu et al.,1997). The rainfall estimates in PERSIANN algorithm are available at 0.25 of spatial resolution for the latitude band 60N-60S from 01/01/1983 to 12/31/2015 (delayed present).

- The latest version of TRMM product (3B42V7) was developed by the National Aeronautics and Space Administration (NASA). This product was obtained from the TRMM Multisatellite precipitation analysis (TMPA) algorithm which combines Infrared (IR) and Passive Microwave (PM) data retrievals. TRMM rainfall estimates incorporates gauge data for bias correction from several sources including national and regional meteorological services. The TRMM-34B2 datasets contain a gridded, TRMM-adjusted, merged infrared precipitation (mm/hr) and RMS precipitation-error estimate, with a 3-hour temporal resolution and 0.25-degree spatial resolution.

- GPCP 0.5 degre V3.1 : The Global Precipitation Climatology Project (GPCP) is a community-based activity of the Global Water and Energy Exchange (GEWEX) project in the World Climate Research Programme (WCRP). The latest release, labeled V3.1, represents a significant improvement over the V3.0 and is considered stable but has

known limitations. The GPCPV3.1 dataset provides a gridded (Level 3) homogeneously processed record of global precipitation estimates at 0.5° spatial and monthly temporal resolution. The current data span is (1983-2019) for the monthly and (June 2000-December 2019) for the daily with the potential to extend this record in the future. Inputs consist of GPM IMERG in the span 55°N-S, and TOVS/AIRS estimates, adjusted climatologically to IMERG, outside 55°N-S. The Daily estimates are scaled to approximately sum to the Monthly value at each 0.5° grid box.

- TARCAT v3.1 is produced by TAMSAT (the Tropical Applications of Meteorology using SATellite data and ground-based observations) research group of the University of Reading and is based on Meteosat TIR CCD. TAMSAT rainfall estimates are provided at 0.0375 x 0.0375 degree spatial resolution (4km) for all land points on the African continent, including Madagascar. Data are are available from Jan 1983 to near-real time at daily , pentadal (5-day), dekadal (10-day) , monthly, seasonal (Dec-Feb, Mar-May, Jun-Aug, Sep-Nov) time steps.

Figure 2.4. shows an overview of all data used in this study. It is a visual and spatial representation of the mean annual precipitation (2001-2014) for the ARC, CHIRPS, PERSIANN, RFE, TARCAT, TRMM 3B42 and TRMM 3B42 datasets and gauges. The general north-south gradient of precipitation was captured by all analysed datasets.

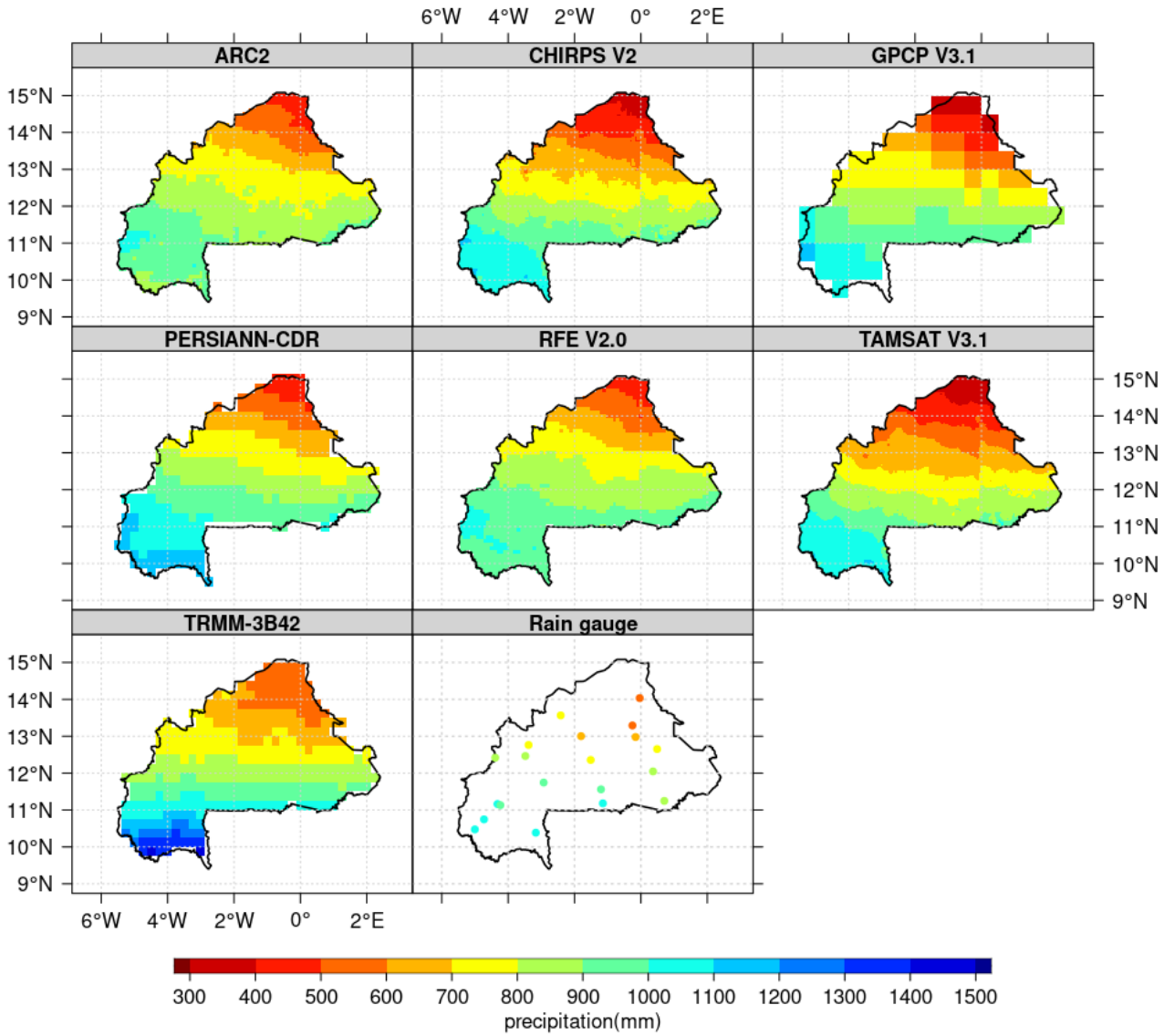

Figure 2.4: overview of mean yearly precipitation of seven Satellite-based precipitation datasets and stations data from 2001 to 2014.

Table 2.1: Summary of selected satellite rainfall datasets for this study

Satellite Databases	Temporal and Spatial resolution	Temporal coverage	Spatial coverage	Type of data	References	Link
PERSIANN-CDR	Daily (0.25°∼27km)	1983 to present	Near global	Satellites, Gauge	Ashouri et al.2015	https://chrsdata.eng.uci.edu/
TAMSAT V3.1	Dekadal, daily,monthly (0.0375°∼4km)	1983 to present	Africa	TIR, gauge	Maidment et al.2014	http:/iridl.ldeo.columbia.edu/SOURCES/
TRMM 3B42	3hourly,daily (0.25°∼27km)	1998 to present	Near global	TIR, VIS, MW, radar, gauge	Huffman et al.2010	https://disc.gsfc.nasa.gov/datasets $TRMM_3B42_Daily_7/$
ARC V2.0	Daily,monthly (0.1°∼10km)	1983 to present	Africa	Satellites, Gauge	Novella et al 2013	http:/iridl.ldeo.columbia.edu/SOURCES/
RFE V2.0	Daily (0.1°∼10km)	2001 to present	Africa	Satellite, gauge	Herman et al.1997	http:/iridl.ldeo.columbia.edu/SOURCES/
CHIRPS V2.0	Daily (0.05°∼5km)	1981 to present	Near global	Satellite, Gauge	Funk et al.2015	http:/iridl.ldeo.columbia.edu/SOURCES/
GPCP L3V3.1	Daily,monthly (0.5°∼50km)	1983 to 2019	Global	PMW-IR-Rain gauge	Huffman et al.2021	https://disc.gsfc..nasa.gov/datasets?keywords.=GPCP%203.1&page=1

2.3 Tools

The various analyses required the use of several tools. These tools were used for data downloading, data processing, formatting, plotting, statistical calculations etc. A brief description of these tools is as follows:

- Python programming language: Python is an interpreted, object-oriented, high-level programming language with dynamic semantics. Python libraries: Numpy, Pandas, Matplotlib,
- R programming language: R is a programming language and open-source software for statistics and data science supported by the R Foundation for Statistical Computing. Libraries used: openair, CDT. . .
- Climate Data Operator: CDO is a collection of command line operators for manipulating

and analyzing climate and NWP model data. Supported data formats are GRIB 1/2, netCDF 3/4, SERVICE, EXTRA and IEG.

- Bash script: A Bash script is a plain text file that contains a series of commands. These commands are a mixture of commands that we would normally type ourselves on the command.
- QGIS: Quantum GIS (QGIS) is an open-source geographic information system (GIS) that implements a wide range of functions for accessing, viewing, displaying, editing, printing and analyzing geospatial data.

2.4 Methods

The different steps for providing an improved gridded rainfall dataset are described in the following flowchart (figure 2.5):

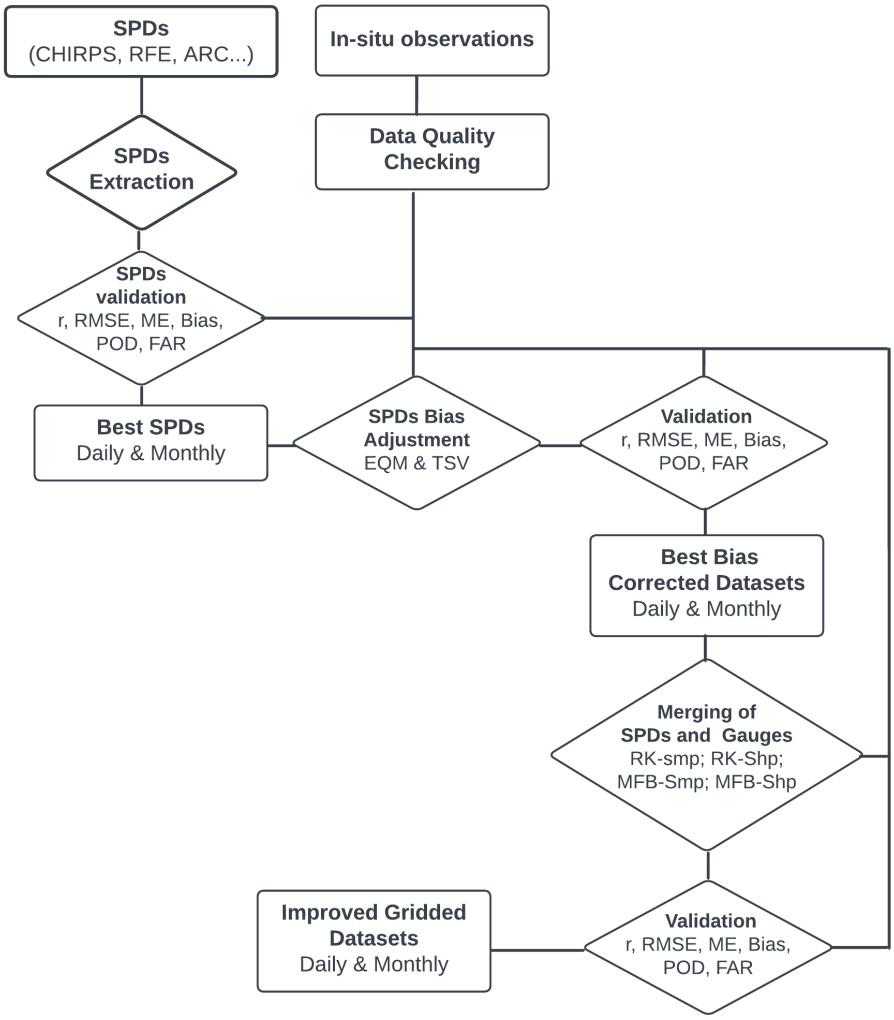

Figure 2.5: Flowchart of the Methodology

Methodology Overview

1. The first step: SPDs the gridded data is extracted at stations location so that at each station location we have two types of data: the satellite data and rain gauge data. This way of doing evaluation has been used rather than interpolating the gauge measurements into a gridded data sets which could result in high biases (Dembélé and Zwart 2016).

2. Then, the series from station data and extracted from gridded are used to compute the validation performances such as below (3.4.1.2). At the end of this step, the best SPDs for each time scale should be identified.

3. In the third step the systematic biases in best-performing SPDs will be removed with the empirical Quantile Mapping (EQM) and Time and space-variant (TSV) approaches.

4. Finally the Regression kriging (RK) and the Mean Field Bias (MFB) algorithms will be applied to blend the bias-adjusted SPDs and rain gauge sets.

2.4.1 Validation of Satellite precipitation datasets

2.4.1.1 Validation process

Verification methods were based on continuous statistics, categorical statistics and the taylor diagram. The continuous validation statistics chosen in this study are: root mean square error (RMSE), standard deviation, and Pearson correlation (r), bias, mean absolute error). Categorical statistics include Probability of Detection (POD) and False Alarm Rate (FAR). All these statistical indicators are well known to be very effective in the evaluation of Satellite precipitation datasets. In summary, the implementation of verification statistics makes it possible to assess how SPDs differ from reference data. All statistics will be calculated for pair comparisons (SPDs and rain gauges). Some of the above statistics, such as the centered root mean square error (centered RMSE), standard deviation (Sd), and Pearson's correlation (r), are summarized in Taylor's diagram (Taylor, 2001). This diagram is necessary for a visual evaluation, especially in situations where the comparison is made between several SPDs. Taylor (2001) uses these statistics to represent the degree of similarity between two sets of data. One dataset will be called "reference" which is the observation data from rain gauges and another dataset represents the estimates or models. The objective is to quantify the degree of resemblance between the estimates and the reference data.

2.4.1.2 Validation Statistics

Person's Correlation (r)

Pearson's coefficient (r) is an index reflecting the strength of the association (a linear relationship) between two continuous variables. For example in this study, it indicates whether the satellite-based estimates match the gauge-based observation. The value of r varies from -1 to 1 (In the

Taylor Diagram r ranges from 0 to 1). The two extreme values respectively indicate that there is a strong positive and negative relationship between two variables. The value 0 means that there is no relationship between the two variables. The formula is given in the equation (2).

Formula		Explanation
$r = \frac{\sum_{i=1}^{i=N} (G_i - \bar{G})(S_i - \bar{S})}{\sqrt{\sum_{i=1}^{i=N} (G_i - \bar{G})^2 \sqrt{(S_i - \bar{S})^2}}}$	(2)	***Gi*** is gauge rainfall measurement, ***Si*** is satellite rainfall estimate, ***N*** is the number of data points, $\bar{G}$ and $\bar{S}$ are the average of gauge rainfall measurement and satellite rainfall estimate respectively.

The root mean square error (RMSE)

The root mean square error (RMSE) is the standard deviation of the residuals (equation 3). Residuals are a measure of how far from the regression line data points are; RMSE is a measure of how to spread out these residuals. In other words, it tells you how concentrated the data is around the line of best fit. RMSE is considered an excellent general purpose error metric for numerical predictions. It is the most famous error metric used in precipitation and rainfall verification studies. The RMSE is always positive and a value of 0 (rarely achieved in practice) would indicate a perfect fit to the data. A smaller RMSE value indicates better accuracy than a higher RMSE value. RMSE has a direct relationship with the correlation coefficient. In other words, if the R Pearson is 1, the RMSE will be 0, because all of the points lie on the regression line, indeed there are no errors.

Formula		Explanation
$RMSE = \sqrt{\left(\frac{1}{N}\sum_{i=1}^{N} (S_i - G_i)^2\right)}$	(3)	***Gi*** is gauge rainfall measurement, ***Si*** is satellite rainfall estimate, ***N*** is the number of data points,

Mean Error (ME)

The Mean Error(ME) is the average of all the errors in a set, see equation (4). An "error" in this context is an uncertainty in a measurement, or the difference between the measured value (satellites data) and "true" value (rain gauge data).

Formula		Explanation
$ME = \frac{1}{N}\sum_{i=1}^{N}\lvert G_i - S_i\rvert$	(4)	***Gi*** is gauge rainfall measurement, ***Si*** is satellite rainfall estimate, ***N*** is the number of data points,

Standard deviation

The standard deviation is a statistic that measures the dispersion of a dataset relative to its mean (equation 5). It shows you how much your data is spread out around the mean or average. The lower the standard deviation, the closer the data points tend to be to the mean (or expected value). Conversely, a higher standard deviation indicates a wider range of values (more data scatter).

Formula		Explanation
$\sigma = \sqrt{(\frac{1}{N})\sum_{i=1}^{N}(S_i - \bar{S})^2}$	(5)	***Si*** is gauge rainfall measurement or satellite rainfall estimate, for a single position/pixel, ***N*** is the number of data points, $\bar{S}$ are the average of rainfall measurement or satellite rainfall estimate.

The bias

The bias is a measure of how the average magnitude of satellite precipitation compares to the observation of precipitation on the ground. The bias indicates whether the satellite data

overestimated or underestimated the precipitation. A value of 1 is the perfect score. A bias value greater (less) than 1 indicates an overall overestimation (underestimation) by the satellite of precipitation amounts on the ground. The formula is given in the equation (6).

Formula		Explanation
$Bias = \frac{\sum_{i=1}^{N}(S_i)}{\sum_{i=1}^{N}(G_i)}$	(6)	***Gi*** is gauge rainfall measurement, ***Si*** is satellite rainfall estimate, ***N*** is the number of data points.

Probability of Detection (POD)

Probability of Detection (POD) indicates what fraction of the rainfall occurrences are correctly detected by the considered satellite algorithms. A higher POD value (equal to 1) means the analyzed dataset can represent all occurrences and 0 means no occurrences are detected (Conti et al., 2013). The formula is given in the equation (7).

Formula		Explanation
$POD = \frac{H}{H+M}$	(7)	H is number of hits, *M* is the number of misses

The False Alarm Ratio (FAR)

The False Alarm Ratio (FAR) indicates what fraction of the number of rainfall occurrences detected by the considered estimation datasets when the reference dataset is not indicating rainfall. The FAR value close to 0 means satellite estimates do not reproduce any false occurrences and 1 if all registered occurrences do not correspond to observed data (Conti et al., 2013). The formula is given in the equation (8).

Formula	Explanation
$FAR = \frac{F}{H+F}$ (8)	F is is number of false alarms H is the number of hits

2.4.2 Bias adjustment

In this study, daily and monthly precipitation were the main variables subject to bias correction. The objective is to adjust the gridded data (satellite rainfall estimates) by the station data. As seen in the literature section, several algorithms are used to correct specific errors in the gridded data. In this study, the best SPDs identified from verification were corrected using two Bias Correction schemes, namely TSV and EQM.

2.4.2.1 Empirical Quantile mapping

To implement the QM method, two empirical CDFs are calculated. The method of calculating empirical CDFs is explained by Wilks.(2011). The QM method adjusts the distribution of daily satellite precipitation (Ps) with the distribution of daily rain gauge precipitation (Po) using a transfer function (h), see equations (9.1 and 9.2). The description of QM is shown in figure 2.6 where the arrow represents the corrections of the QM method.

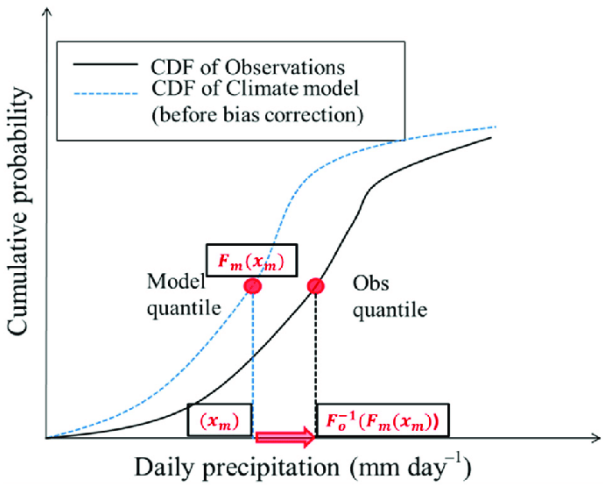

Figure 2.6: Schematic of the quantile mapping method. Adapted from Kim et al.(2016)

Formula		Explanation
$P_C = h(P_S)$	(9.1)	**Ps** is the distribution of precipitation amount to be corrected **Pc** is the corrected precipitation value **h** is a transfer function
$P_C = CDF_G^{-1}(CDF_S(P_S))$	(9.2)	**CDFs** is the daily or monthly CDF of the Satellites estimates CDFG−1 is the inverse of the daily or monthly CDF of the rain-gauge observations

2.4.2.2 Time and space-variant bias correction

The bias correction factor is computed for every gauge station. In this method, it is defined as the ratio of the sum of the gauge observations to the satellite estimations as shown in the equation (10.1). If the bias is assumed to be heterogeneous in space (independent and normally distributed), the bias factor at the station locations is interpolated to the grid of the gridded data using Inverse Distance Weighting (IDW) method (equation 10.2). Finally, the adjusted SPDs are generated by multiplying the entire domain of raw SPDs by this correction factor value interpolated, see equation (10.3). For daily data, a centered time window of 5 days will be added to take into account the variability.

Formula		Explanation
$BF_{tj} = \frac{\sum_{i=t\ for\ each\ year}^{N} (G_{tj})}{\sum_{i=t\ for\ each\ year}^{N} (S_{tj})}$	(10.1)	**t** is the time period 1 to 365 for daily and 1 to 12 for monthly data **BFtj** is the bias factor for daily or monthly denoted as t at a station j **Gtj** is the value at the station j for the time t **Stj** is the value of the satellite gridded data at the station j for the time t
$A' = IWD(BF_{tj})$	(10.2)	**A'** is the value of multiplicative correction factor for each pixel **IDW** is inverse distance weighted interpolation method
$P* = A' \times P$	(10.3)	**P*** is the corrected precipitation value **P** satellite value to be corrected

2.4.3 Merging Approach

This section is the final step in the process of producing the improved dataset in terms of spatial and temporal resolution and accuracy. It consisted of combining the bias-corrected datasets with the ground observations. Based on the literature review, in terms of performance and widespread use, this study proposed to apply the Mean Field Bias method of bias adjustment category, and regression kriging also called "kriging after detrending" from the integration category. MFB remains one of the most widely used merging methods for operational applications and by many national meteorological services (Goudenhoofdt and Delobbe, 2016). The two methods need to be compared in the context of Burkina Faso to provide conclusive evidence of their relative performance. Then, two interpolation methods were each applied to these mixing methods. Shepard'method (malvic et al., 2020) and modified Spheremap scheme (Scham et al. 2013 Becker et al., 2013) were used for interpolation. In summary, four approaches were selected for the satellite-gauges combination in this study. A description of these methods is given in the next sections.

- Regression kriging with Spheremap (RK- Spheremap)
- Regression kriging with Shepard (RK- Shepard)
- Mean Field Bias with Spheremap (MFB - Spheremap)
- Mean Field Bias with Shepard (MFB- Shepard)

2.4.3.1 Regression-kriging

Regression kriging is a spatial interpolation technique that combines regression of the dependent variable (target variable) on the predictors with kriging of the prediction residuals. In other words, regression kriging is a hybrid method that combines a deterministic model (a simple or multiple linear regression model) with (a statistical model) ordinary kriging of prediction residuals (Odeh et. al., 1995; Goovaerts et al., 1997). In the case of the blending of satellite and rain gauge data, the deterministic or regression model consists of estimation by modeling the relationship between the target (station data) and auxiliary (satellite data) environmental variables at the sample locations and applying it to ungauged locations. Next, the statistical method performs the interpolation of regression residuals at station locations over the entire grid using ordinary kriging. Finally, RK combines these two approaches: statistical adjustment and

modeling (Hengl et al., 2007; De Vera et al., 2021). the first part of the right side of equation (11.1) represents the regression and the second part represents the kriging of the residual.

Formula		Explanation
$\hat{z}(s_0)=\hat{m}(s_0)+\hat{e}(s_0)$	(11.1)	**m(So)** is the fitted deterministic part **ê(So)** is the interpolated residual
$\hat{z}(s_0)=\sum_{k=1}^{p}\hat{\beta}_k.q_k(s_0)+\sum_{i=1}^{n}\lambda_i.e(s_i)$	(11.2)	**βk** are the estimated deterministic model coefficient **qk(So)** is the kth predictor at location So **λi** are the kriging weights determined by the spatial dependence structure of the residual **e(Si)** is the residual at the position Si
$q_0(s_0)=1$		

2.4.3.2 Mean field bias

Mean-field bias technique has been widely used for merging radar and gauges data. It became a standard method of merging satellite estimates and gauges data. Mean Field Bias (MFB) correction assumes the existence of a uniform multiplicative error in the field of the satellites. A simple multiplicative factor is therefore used to uniformly correct the domain of the satellites. It is then multiplied at each pixel of the precipitation estimates by remote sensing. The correction factor in this method is defined as the ratio of the sum of the gauge observations to satellites estimates (equation 12):

Formula		Explanation
$C_{MFB}=\frac{\sum_{i=1}^{N}(G_i)}{\sum_{i=1}^{N}(S_i)}$	(12)	***Gi*** is gauge rainfall measurement, ***Si*** is satellite rainfall product, ***N*** is the number of valid rain gauge.

Chapter 3

Results and Discussion

3.1 Results

3.1.1 Validation of Satellite-Based Precipitation Datasets

The performance of the SPDs was assessed at different spatial (for each climate zone) and temporal (daily and monthly) scales over the period 2001-2014. The metrics calculated and presented in the tables are not calculated in the same way as those in the Taylor diagram. In the tables, all metrics are calculated for each station before the average per metric is calculated. In the Taylor diagrams, in addition to incorporating the standard deviation, the averages of the daily and monthly data were first calculated before calculating the metrics. The scatter plots showing the distribution of satellite and rain gauge data are given in appendix 1 and appendix 2.

3.1.1.1 Validation at daily time scale

Most of the SPDs performed poorly on daily rainfall estimates. The statistics used to compare the rain gauge data with the seven satellite data sets are presented in Table 3.1. Considering the 8 missing days in the ARC2 and one day in the RFE, the number of value pairs compared over 14 years is 5104. Thus the validation carried out by climatic zone is as follows:

- **The Sahelian Zone**
  Over the Sahelian zone, all SPDs overestimate rainfall (bias>1), except for CHIRPS and PERSIANN-CDR which underestimate it, see Table 3.1.a. The ARC2 shows the best correlation (r = 0.807). The best bias (0.975) and worst correlation (0.622) are observed

with CHIRPS while the worst bias is for RFE (1.132). PERSIANN has the highest value of RMSE (3.307) and FAR (0.289). The smallest FAR (0.203) is for GPCP. The TAMSAT presents the best score for the RMSE (2.418) and POD (0.737) while TRMM-3B42 has the worst POD. Summarising all the statistics, it appears that TAMSAT is the most efficient in reproducing precipitation in the Sahelian zone followed by RFE. GPCP showed the worst performances.

- **The Soudano-sahelian Zone**
  The SPDs that overestimate and underestimate rainfall in the Sudano-Sahelian zone are the same as those in the Sahelian zone (Table 3.1.b). CHIRPS shows the best bias (0.974) and the lowest correlation (0.690). The GPCP has the lowest performance for the bias (1.117), the RMSE (3.675), and the POD (0.752). The worst FAR (0.208) and best POD (0.821) are for PERSIANN-CDR. On the other hand, TAMSAT shows the best score for the correlation (r=0.869) and the RMSE (2.116). The best FAR (0.13) is shown by TRMM-3B42. Based on these statistics the TAMSAT database is also the most appropriate database for the Sudano-Sahelian zone.

- **The Soudanian Zone**
  In this zone of Burkina Faso, according to Table 3.1.c, all SPDs underestimated the rainfall amounts (bias<1). ARC2 presented the best correlation (r = 0.308) and the worst bias (0.715), while CHIRPS has the worst performances for the correlation (0.242) and also for POD (0.742). The best bias (0.828) and the worst RMSE (12.646) are shown by GPCP. The best RMSE (12.201) is for TAMSAT. PERSIANN-CDR shows the best POD (0.817) and the worst FAR (0.218). TRMM-3B42 has the best FAR (0.120). In short, TAMSAT has the best performance of all the others in the Sudanian zone followed once again by RFE.

The Taylor diagram (Figure 3.1) is plotted by considering the spatial average of the daily precipitation values of the stations in each climate zone. The Taylor diagram (Taylor, 2001) summarizes the geometric relationship between the correlation coefficient, the standard deviation of the series, and the centered root mean square error. Statistics for eight models were computed, and color was assigned to each SPD considered. The position of each point appearing on the plot quantifies how closely that SPD matches observations. In the Sudanian zone, the SPDs show very poor performance compared to the other zones with correlations less than 0.65 and centered mean square errors greater than 0.85 mm/day. TAMSAT datasets have shown the best agreement with rain gauge data in all climatic zones, followed by RFE. However, GPCP showed the weakest performance. The diagram confirms therefore the results of table 3.1.

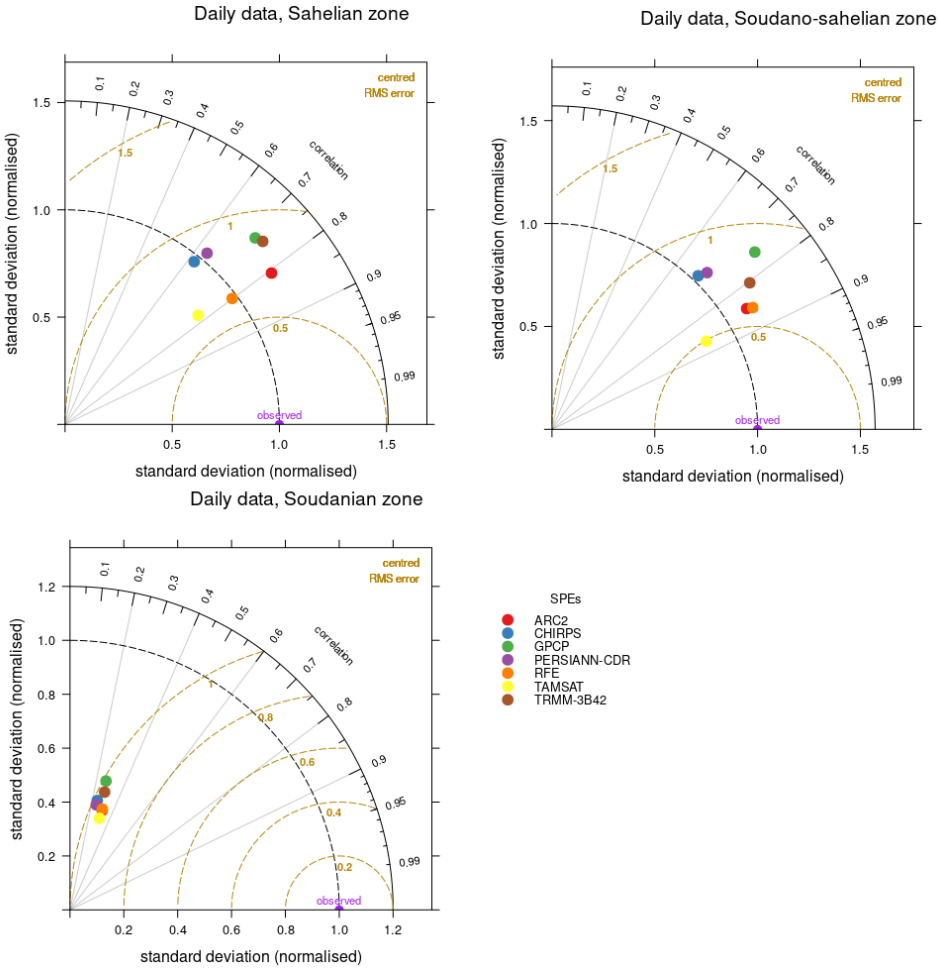

Figure 3.1: Taylor diagram for the three climatic zone obtained from spatial averaged of daily data

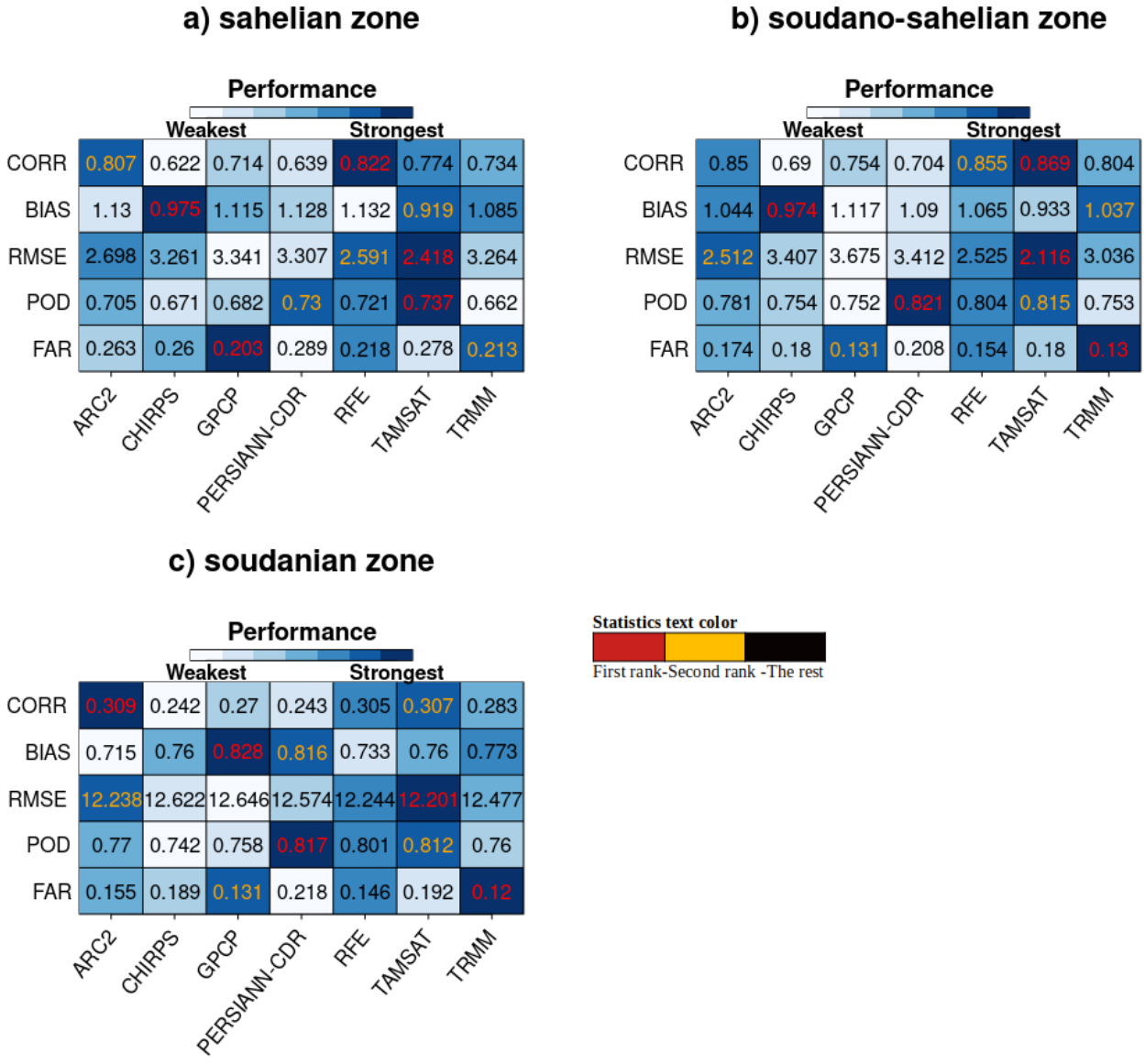

Table 3.1: Statistical indicators for daily time scale

3.1.1.2 Validation at monthly time scale

Monthly validation was also performed using the same statistical approaches as for the daily time scale. The performance of all Datasets in capturing observed precipitation was better at the monthly scale than the daily scale. Statistical metrics such as POD and FAR were not computed for the monthly time scale, as they aim to assess the abilities of the SPDs to capture the occurrence of events which are less significant for the monthly time scale. Table 3.2 summarizes the performance of the SDPs. The number of pairs of values compared over the 14 years is 168, which means that no missing months were recorded.

- **The Sahelian Zone**
  All SPDs overestimate the amount of rainfall (Bias > 1) except CHIRPS and TAMSAT which underestimate it (Bias< 1). The SPDs correlated well compared to daily time scale with correlation coefficient values ranking from 0.966 to 0.984; Bias didn't show major changes (0.976 to 1.131) compared to daily time scale, see table 3.2.a. On the other hand, RMSE values at monthly scale show high values from 11.371 to 18.005. The best score for correlation (0.984), Bias (0.976) and RMSE (11.371) were observed for CHIRPS. While TAMSAT has the worst performances for correlation (0.966) and the RMSE (18.005). RFE presents the worst bias (1.131). To summarize, CHIRPS has the best performances for the Sahelian zone.

- **The Soudano-sahelian Zone**
  The SPDs that overestimate and underestimate rainfall in soudano-sahelian zone are the same as those in Sahelian zone, see table 3.2.b. The best Bias (0.934), RMSE (9.454) were presented by CHIRPS. However the the worst scores for the Correlation (0.98), and the RMSE (17.131) have been detected with ARC2. GPCP has the worst bias (1.097) and the best correlation (0.994). Based on these performances, CHIRPSV2 has the best agreement with gauge data over Soudano-sahelian Zone.

- **The Soudanian Zone**
  The PERSIANN-CDR and GPCP overestimated rainfall amount (bias<1) (table 3.2.c). PERSIANN-CDR exhibited the best scores for all metrics (corr=0.988; bias=1.017;RMSE=13.658) whereas ARC2 performed poorly. PERSIANN-CDR, therefore is the most suitable for this zone.

The Taylor diagram, drawn by considering the spatial average of the monthly precipitation values, is presented in Figure 3.2 very close points are observed in all the climatic zones compared to

figure 3.1. This indicates a high precision in the estimation of the monthly data than the daily ones. The analysis of the monthly Taylor diagram indicates that CHIRPS presents the best performances in the Sahelian and Sudano-Sahelian zone followed by TRMM-3B42. In the Sudano-Sahelian zone, PERSIANN-CDR is the most efficient followed by CHIRPS.

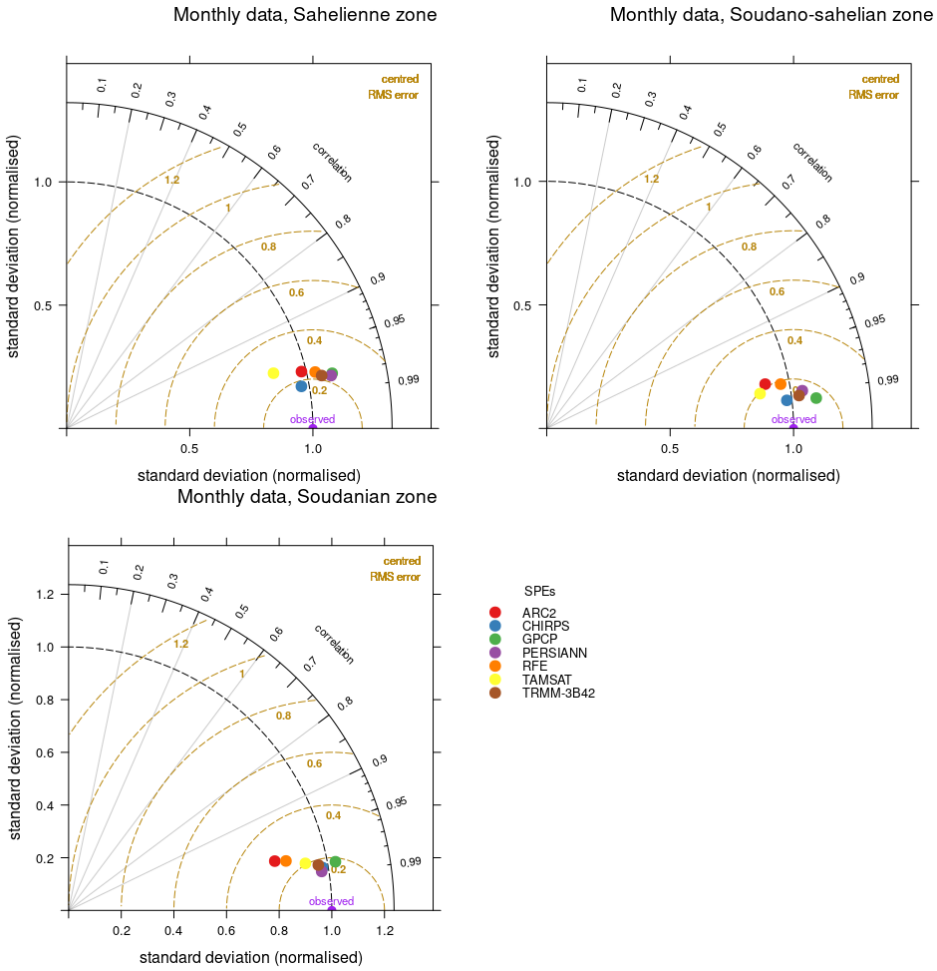

Figure 3.2: Taylor diagram for the three climatic zones obtained from spatial averaged of monthly values.

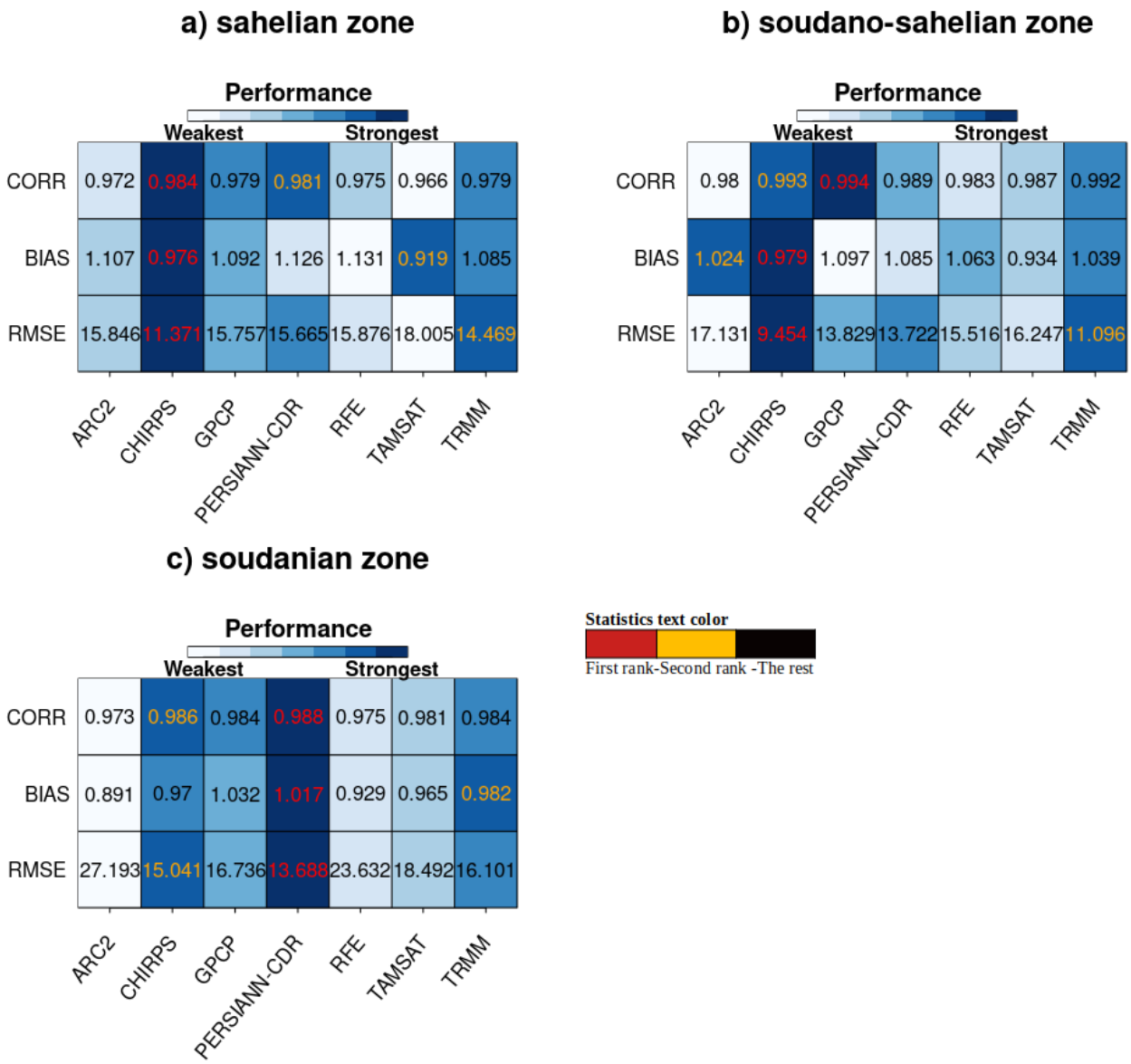

Table 3.2: Statistical indicators for monthly time scale

Figure 3.3 shows the comparison between the average amounts of precipitation per month of the 97 stations selected for this study (reference) with the Seven satellite estimate datasets. All seven capture precipitation patterns considerably well, especially the peak of precipitation in August. During the dry season (October to April), almost all satellite rainfall datasets tend to overestimate the amount of rainfall. During the rainy season (May to September), they underestimate it except PERSIANN-CDR and GPCP. ARC2 is the one that underestimates the most and therefore the least effective. However, CHIRPS and PERSIANN-CDR show relatively better skills compared to others.

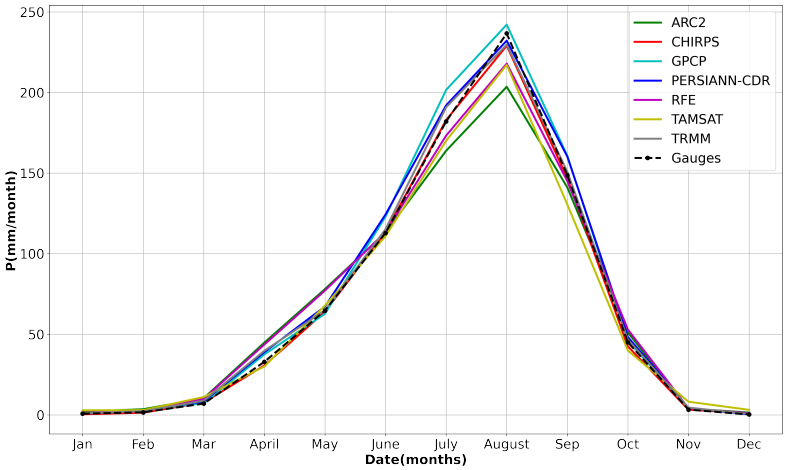

Figure 3.3: Comparison of monthly precipitation captured by satellites precipitation estimates datasets with rain gauge.

3.1.2 Bias Adjustment of Satellite-Based Precipitation Datasets

Two SPDs were adjusted using two bias adjustment methods: the choice of these SPDs was based on the validation of the seven SPDs above (section 4.1.1). Therefore, TAMSAT V3.1 and CHIRPSV2 datasets were used for daily time scale and monthly timescale respectively. The application of two bias adjustment approaches aims to determine the most effective, i.e the one that best reduces the systematic errors of the SPDs for the study area.

3.1.2.1 Analysis of bias adjustment methods for daily rainfall accumulations

Table 3.3 presents the 14-year average values of bias, RMSEs, MEs, and CORRs of the original TAMSAT datasets, TAMSAT bias-corrected datasets with empirical quantile mapping (EQM)

and time spatial variant (TSV). these metrics show that the quality of two bias corrected datasets has been improved over uncorrected. The EQM outperforms the TSV on all metrics except FAR: its correlation is much better (0.286) against 0.15 for the TSV. It also shows superior performance in terms of ME, Bias, RMSE and POD. However, its FAR (0.589) is slightly lower than that of TSV (0.581). The bias correction approaches are both necessary and effective, but EQM is remains the best for daily data. It has improved the correlation coefficient by 94.5% (from 0.147 to 0.286), the Bias by 10.3% (from 0.875 to 0.965) and the RMSE by 3.0% (from 26.494 to 25.708).

Taylor diagram (Figure 3.4) is also used to find out how well the corrected datasets match the gauge-based precipitation. EQM has improved significantly the correlation (around 0.88) and centered root mean square error (0.5). The EQM corrected dataset is followed by the TSV corrected dataset in terms of performance, which shows a slight improvement over the uncorrected dataset.

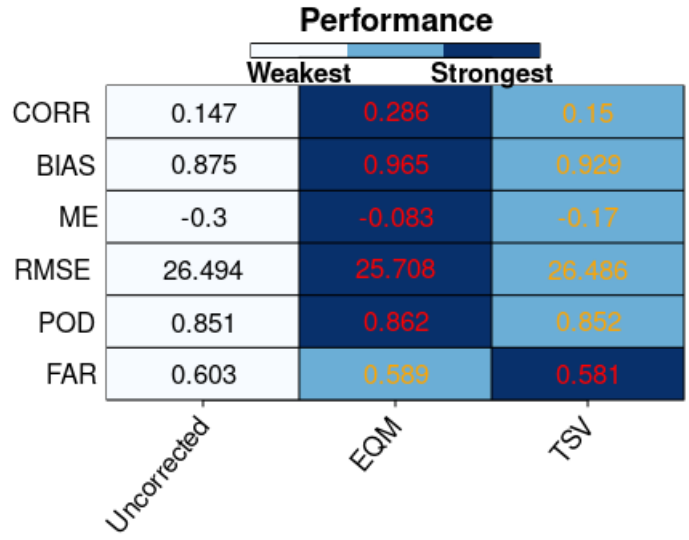

Table 3.3: Summary of daily bias correction statistical indicators

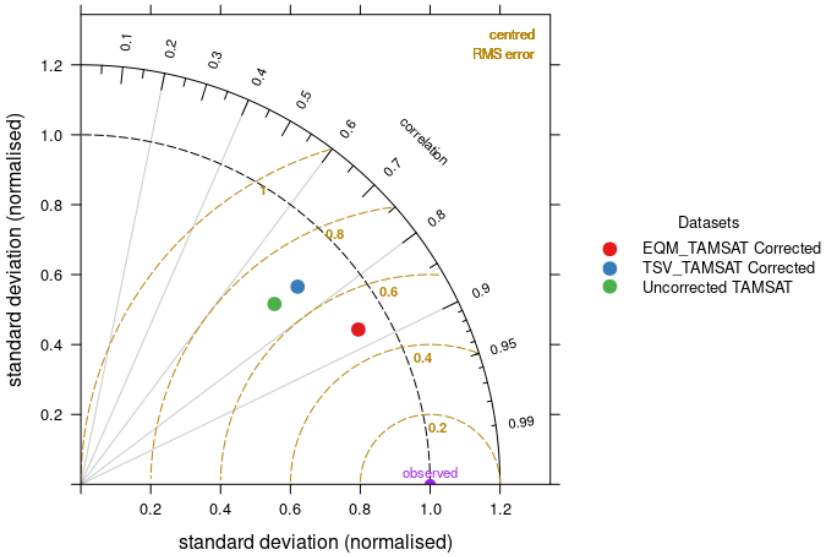

Figure 3.4: Taylor Diagram of daily data spatial average

Figure 3.5.a compares daily average rain gauge data with uncorrected TAMSAT datasets. TAMSAT dataset captures the rainfall trend observed during the dry season. But it underestimates the amount of precipitations from 200 to 260 days (Julian days) "wet months". In November (300 to 330), the rainfall is also systematically underestimated. Figure 4.5.b then compares the average daily rain gauge data with the Bias corrected TAMSAT datasets using EQM. This figure shows slight improvements in the overestimation of rainy days compared to the figure 3.5.a.

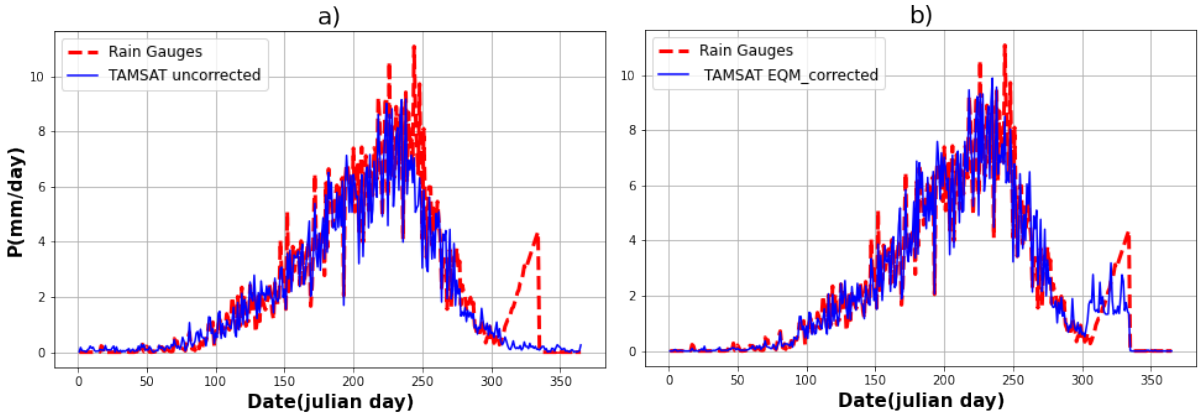

Figure 3.5: Comparison of daily average rain gauge data with uncorrected TAMSAT and bias-adjusted TAMSAT datasets over the period 2001-2014.

3.1.2.2 Analysis of bias adjustment methods for monthly rainfall accumulations

The performances of bias corrected datasets with EQM presented in Table 3.4. According to these metrics, the two bias correction methods added value to the uncorrected dataset. Comparing the methods, the dataset corrected with TSV has a slightly better correlation (0.921), bias (1.001), ME (0.046) and RMSE (34.686) than those of EQM, which are in the same order: 0.919, 0.991, -0.598 and 35.058. TSV methods has improved the correlation coefficient by 0.5% (from 0.916 to 0.921), the Bias by 2.4% (from 0.977 to 1.001) and the RMSE by 2.8% (from 35.654 to 34.986).

In the Taylor diagram (figure 3.6), all metrics have been computed based on the monthly mean value. The diagram shows three clustered points very close to each other. The EQM-corrected dataset shows a slightly higher correlation, while the TSV-corrected dataset shows the same standard deviation as the reference. This result, which shows that the EQM is the most effective bias correction being closer to the reference, may seem to contradict the results of Table 3.4. This discrepancy is due to the differences in the methods of calculating the metrics already explained in section 3.1.1.

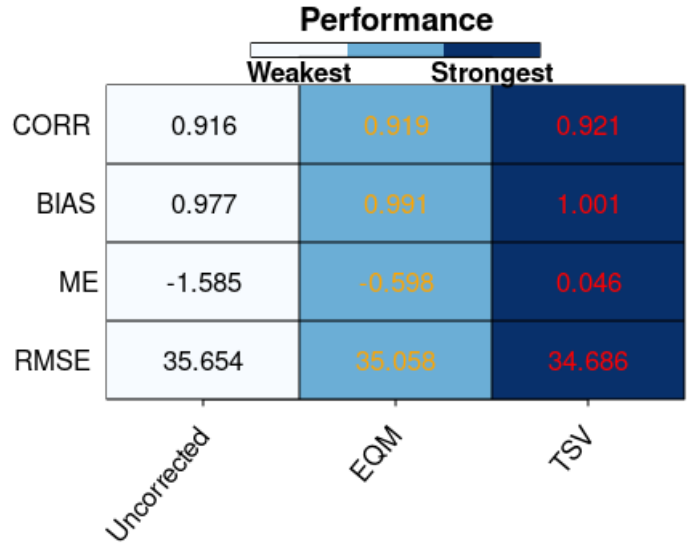

Table 3.4: Summary of monthly bias correction statistical indicators

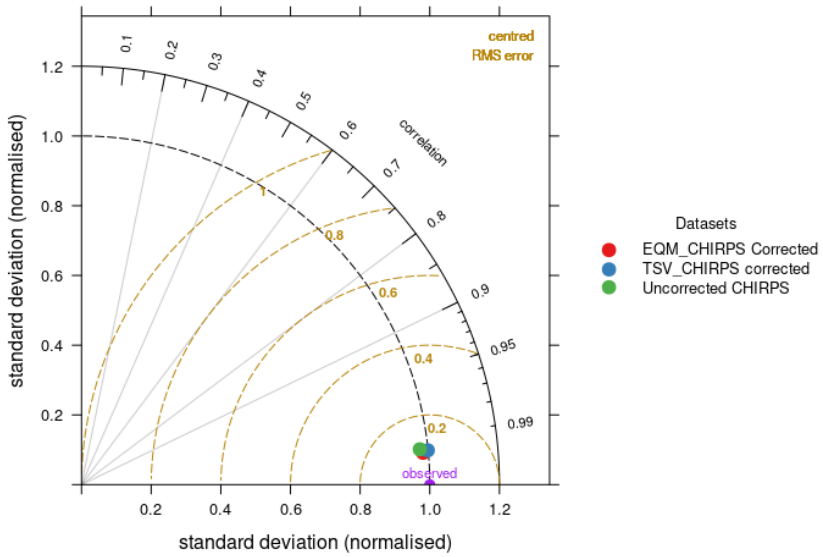

Figure 3.6: Taylor Diagram of monthly data spatial average

Figure 3.7 compares monthly average rain gauge data with uncorrected CHIRPS and bias-adjusted CHIRPS datasets. Although the uncorrected TAMSAT precipitation patterns closely resemble the rain gauge data patterns, it underestimates the July to November "wet months" precipitation (Figure 3.7.a). After the bias correction the two curves are now very similar (Figure 3.7.b). The overestimations during July-October period have therefore been adjusted.

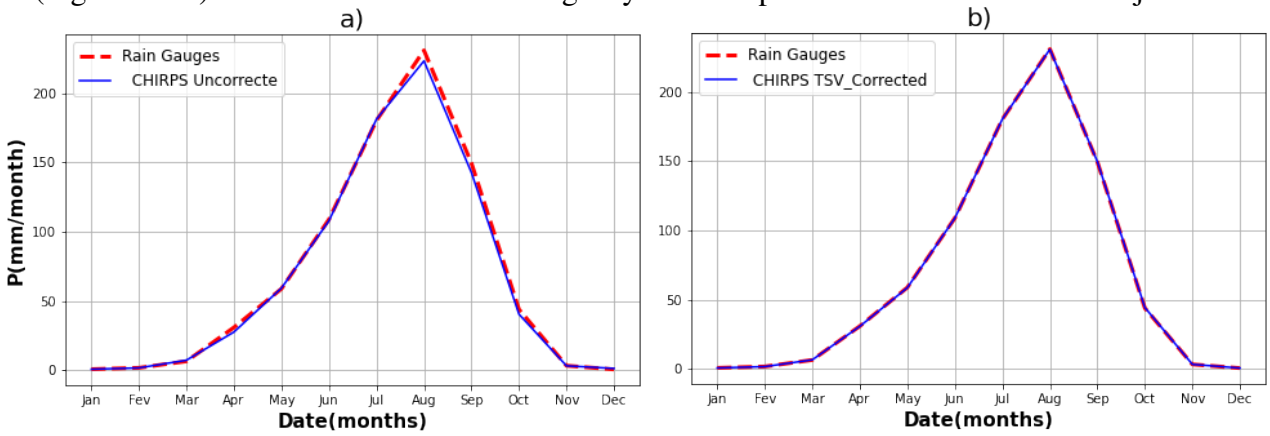

Figure 3.7: Comparison of monthly average rain gauge data with uncorrected CHIRPS and bias-adjusted CHIRPS datasets over the period 2001-2014.

3.1.3 Merging of Satellite-Based Precipitation Datasets

3.1.3.1 Analysis of merging methods for daily Datasets

Table 3.5 presents the performance of the four merged precipitation datasets, assessed using categorical and continuous statistical indicators. As the statistics show, each merging method

reduced all systematic errors compared to the unmerged dataset, which means that they are all effective. They all have a high correlation (0.999). Regression-sphere kriging provided the largest reduction in ME(-0.003), Bias (0.999), RMSE (1.175), FAR(0), and the largest increase in POD (1). It is closely followed by MFB-Spheremap which also shows significant improvements in RMSE(1.201), POD(0.998), and FAR(0). The two methods RK-Shepard and MFB-Shepard perform the worst due to their high scores in RMSE (1.22; 1.208 respectively) and FAR (0.012; 0.005 respectively). The RK-Spheremap merging approach improved the correlation by 71.4% (from 0.286 to 0.999), the bias by 3.4% (from 0.965 to 0.999) and the RMSE by 95.4% (from 25.708 to 1.175).

In the Taylor diagram (figure 3.8), the methods are validated in terms of standard deviation, correlation, and centered RMSE. It shows a very high degree of agreement between merging methods and reference data, with RK-Sphermap regression Kriging being the most reliable.

Figure 3.9 shows a visual overview of the improvement made by merging the bias-corrected datasets with the rain gauge data. In Figure (3.9.a), unmerged dataset shows underestimations of the daily cumulative rainfall in some periods. After merging (Figure 3.9.b) with RK-Spheremap method, they could be corrected and the merged dataset match the rain gauge data quite well.

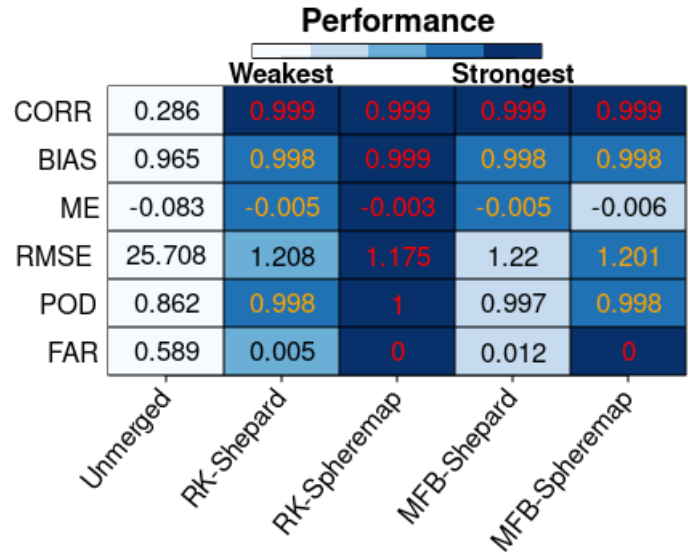

Table 3.5: Summary of daily merging statistical indicators

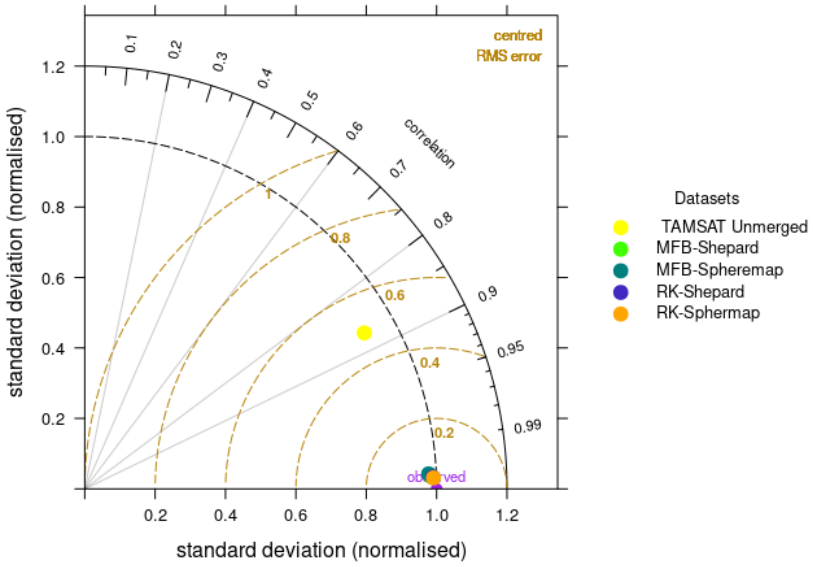

Figure 3.8: Taylor Diagram of daily data spatial average

In the figure 3.10 some examples of days have been considered, one in the dry season and the other in the wet season. The objective is to show through a comparison of rain gauge data, raw TAMSAT data and merged data, the effectiveness of data sets merging. On December 31, 2010 for example, TAMSAT estimated false rains. This could be corrected through the merging of these data and that of the rain gauges. Similarly, the day of July 29, 2010 was rainy, however TAMSAT recorded only low rain. This has also been corrected by merging.

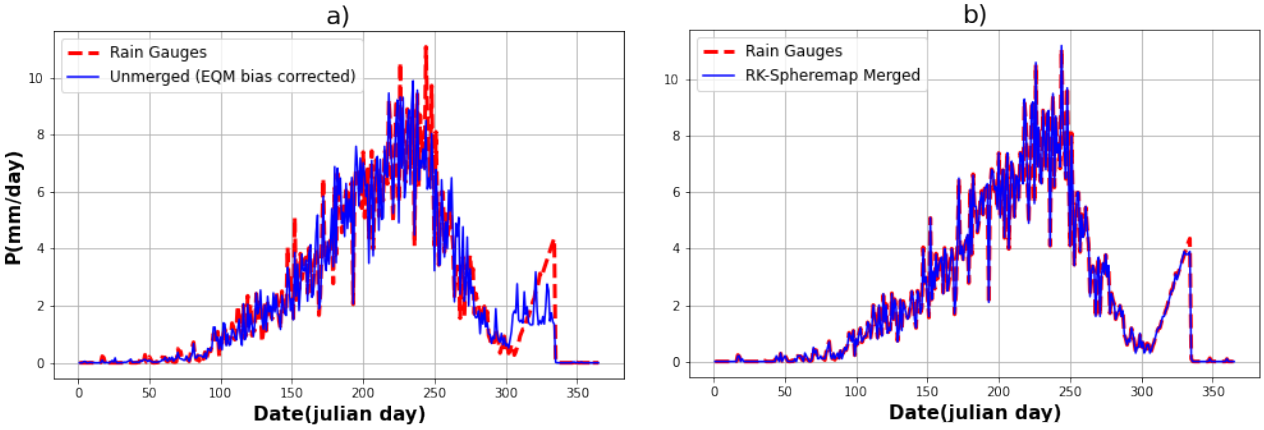

Figure 3.9: Average of daily rain gauges data over 2001–2014, compared to TAMSAT unmerged data and TAMSAT merged

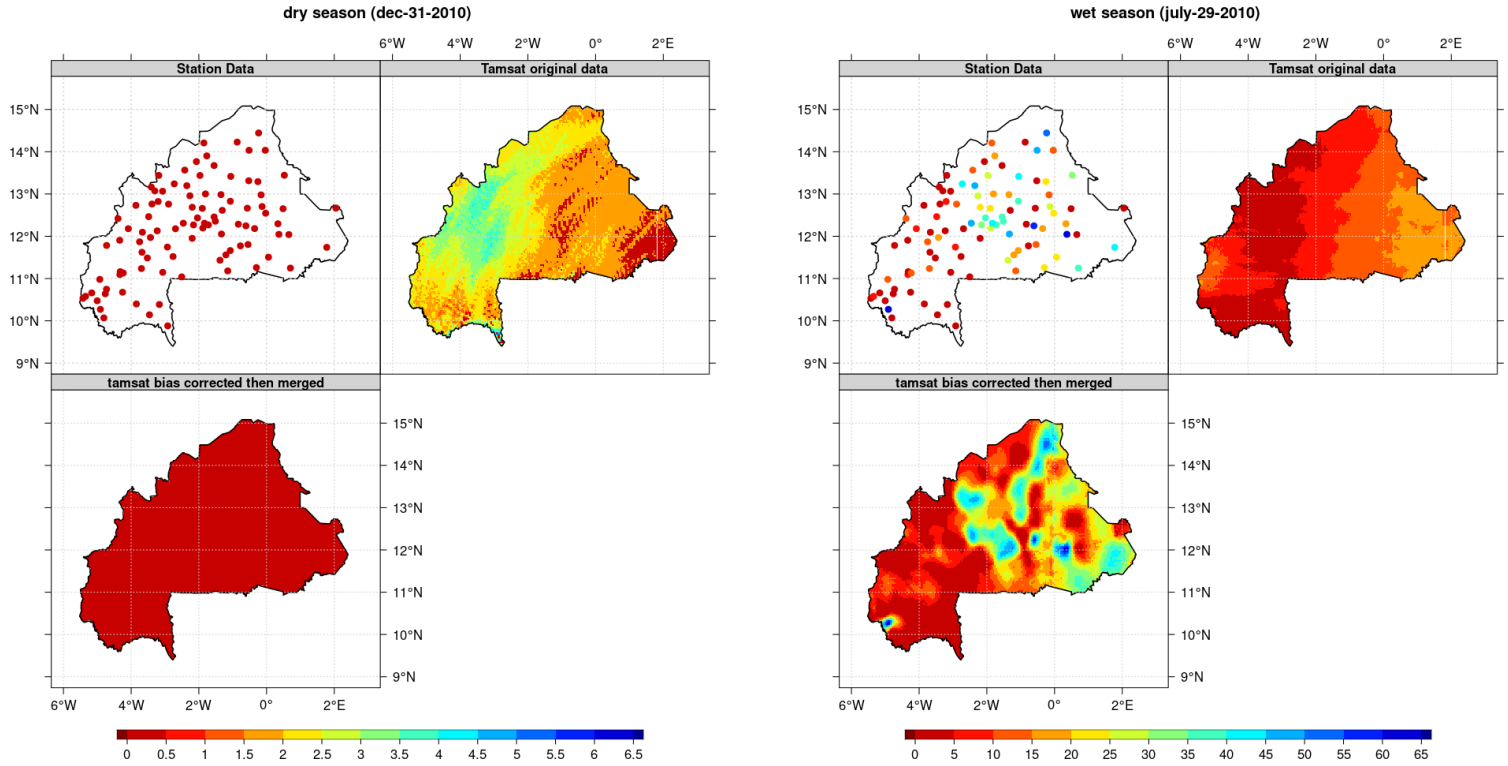

Figure 3.10: Comparison of daily rainfall (mm) for 29 july 2010 and 31 December 2010 between rain gauge, original TAMSAT and final data sets merged

3.1.3.2 Analysis of merging methods for monthly datasets

At the monthly scale, all merging methods generated highly correlated datasets (r =1) with the rain gauge data, and conciderably reduced biases (bias=1), see table 3.6. Regression kriging - Spheremap again outperformed the other methods with the lowest values of ME (0) and RMSE (0.042). It outperformed MFB-Spheremap only because of its low RMSE value. On the other hand, MFB-Shepard remained the worst performer with the highest ME (-0.002) and RMSE (1.306). As previously, the RMSE was significantly reduced in all methods (i.e. 34.686 to less than or equal to 1.306). These results suggest that the Regression Kriging - Spheremap mixture method is the most appropriate for combining rainfall data and satellite estimates. This method improved the correlation coefficient by 7.9% (from 0.921 to 1), the bias by 0.1% (from 1.001 to 1) and the MSE by 99.87% (from 34.686 to 0.042).

The Taylor diagram (Figure 3.11) again confirms the results of Table 3.6 although the methods of calculating the statistics in this diagram are different. It shows completely overlapping points. The correlation of the methods is the same and the values of the standard deviation and the centred RMSE are very close. The RK-Spheremap comes out on top of the other methods although almost all of them perform well.

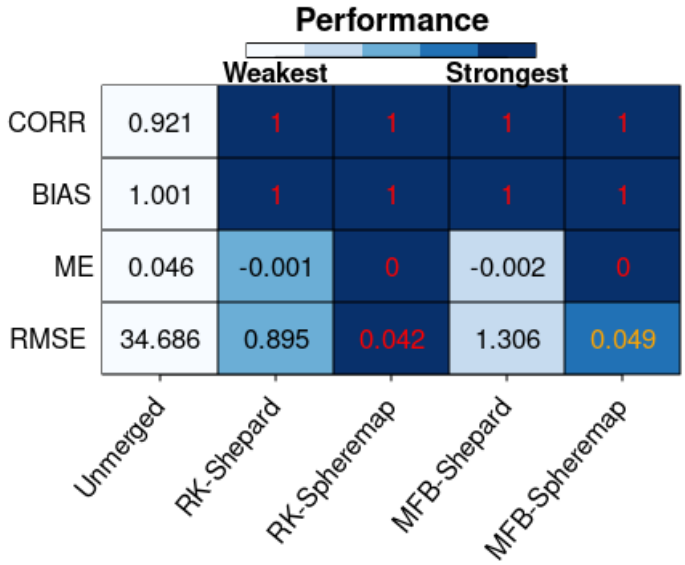

Table 3.6: Summary of monthly merging statistical indicators

Figure 3.12 shows the comparison between the rainfall data and the unmerged data (3.12.a) on

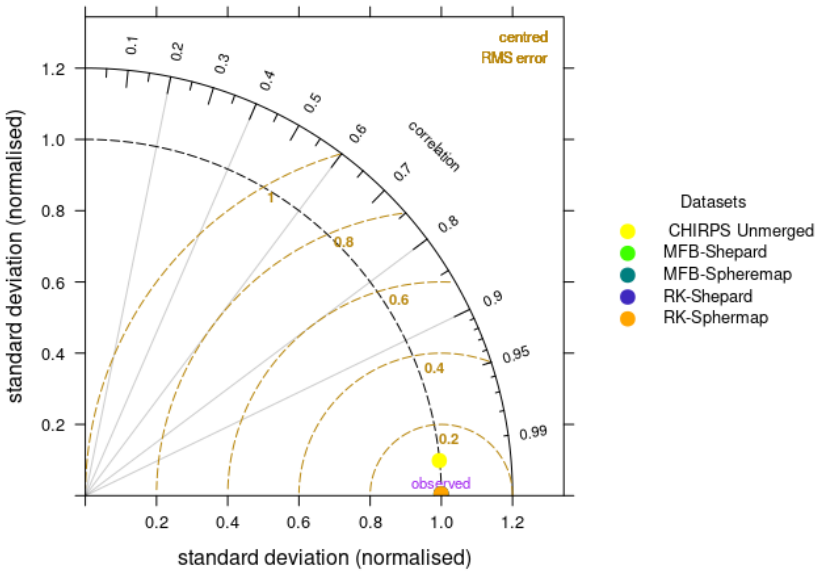

Figure 3.11: Taylor Diagram of monthly data spatial average

the one hand and the rainfall data and my data after fusion on the other hand (3.12.b). The two graphs are very similar. Indeed, after the bias correction, the monthly time series had improved a lot. This is why the graphs do not show any apparent change, however, the statistics have improved according to Table 3.6.

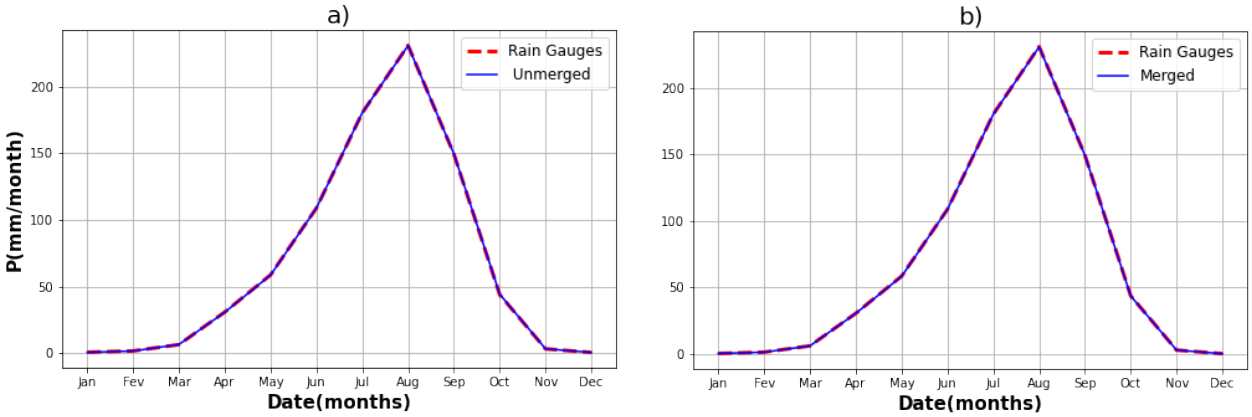

Figure 3.12: Average monthly rain gauges data over 2001–2014, compared to CHIRPS unmerged data and CHIRPS merged

Similar to figure 3.10, some examples of months have been also considered in figure 3.13, one in the dry season and the other in the wet season. In December 2010, TAMSAT estimated false rains. This could be corrected through the merging of these data and that of the rain gauges. Likewise, in September corrections have been made, see figure.

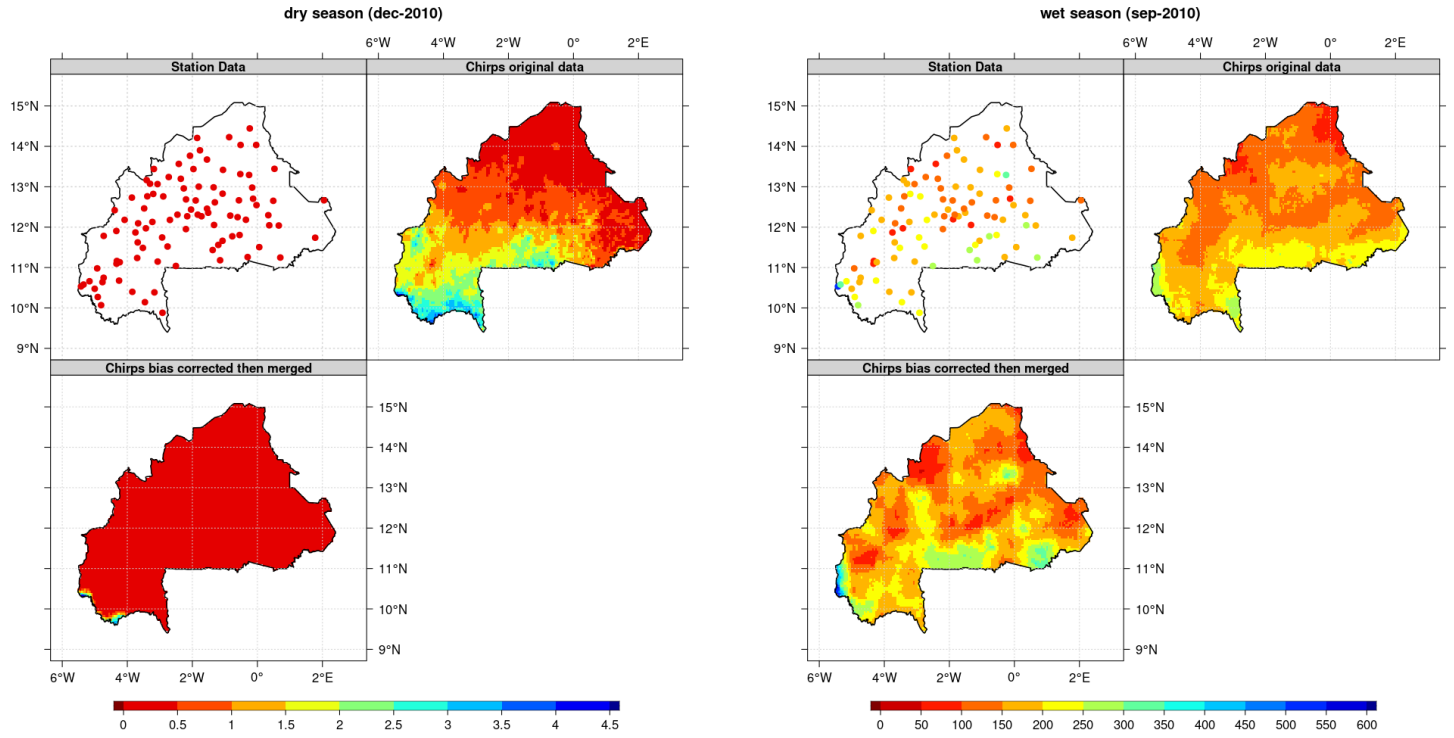

Figure 3.13: Comparison of monthly rainfall (mm) for September 2010 and December 2010 between rain gauge, original TAMSAT, and final data sets merged

3.1.4 Summary of the main results of the study

Table 3.7: Summary of enhancements to the TAMSAT daily dataset for Burkina Faso

	Bias Correction			Merging			Total
Metrics	Original	Bias corr	percen	Bias corr	Merged	percen	percent
CORR	0.147	0.286	**94.5%**	0.286	0.999	**71.4%**	**85.2%**
BIAS	0.875	0.965	**10.3%**	0.965	0.999	**3.4%**	**12.4%**
RMSE	26.494	25.708	**3%**	25.708	1.175	**95.4%**	**95.6%**

Table 3.8: Summary of enhancements to the CHIRPS monthly dataset for Burkina Faso

	Bias Correction			Merging			Total
Metrics	Original	Bias corr	percen	Bias corr	Merged	percen	percent
CORR	0.916	0.921	**0.5%**	0.921	0.999	**7.9%**	**8.4%**
BIAS	0.977	1.001	**2.4%**	1.001	0.999	**0.1%**	**2.3%**
RMSE	35.654	34.686	**2.8%**	34.686	0.042	**99.87%**	**99.9%**

3.2 Discussion

- Evaluation of SPDs.
  According to the analyses, the performance of satellite precipitation datasets for the monthly time step is better than the daily ones. As indicated by previous studies (Dembélé and Zwart 2016), the performance of satellite estimates improves with increasing time steps. Indeed, errors at smaller time scales (overestimates and underestimates) compensate when aggregated to a larger time step. Moreover, the results of the evaluation show that TAMSAT, which performs best on a daily time step, performs less well on a monthly time step. Indeed, for a given database, the algorithms that capture daily events are different from those that capture monthly events. This is why the aggregation of daily data gives different values than the monthly values directly provided by the same database. Therefore, a database may have the best algorithms for daily estimates and the worst algorithms for monthly or seasonal estimates. The results of this study are different from those of Dembélé and Zwart (2016) who also worked on the evaluation of SPDs in Burkina Faso. They found that CHIRPS performed better at the daily time step while TAMSAT performed better in the present study. This discrepancy can be explained by differences in the data used in the two studies. The present study considered 97 stations in the assessment, compared to ten (synoptic) stations in Dembélé and Zwart (2016). Moreover,

the CHIRPS data already contain synoptic station data (i.e. satellite data merged with synoptic stations). Therefore, is therefore logical that an evaluation of the CHIRPS data with synoptic stations as reference shows that CHIRPS is the best. The originality of this evaluation compared to previous studies lies in the consideration of different climatic zones instead of considering the whole country as a homogeneous zone (Beck et al, 2017, Toté et al 2015, Bayissa et al, 2017, Atiah et al, 2020). The validation results of SPDs are very often divergent as the performance of these SPDs is highly dependent on the region and the local climate system as highlighted by some authors (e.g. sun et al 2017).

- Bias correction of SPDs
  Quantile mapping and space-time variable are the two methods applied to the datasets in this study to remove bias. TVS performed poorly on the daily time scale, as it slightly improved Corr, ME, RMSE, Bias and FAR compared to EQM. The high performance of EQM is due to the principle based on empirical cumulative point distribution functions (ecdfs) constructed daily.Therefore, it has the ability to perfectly match the CDF of the daily precipitation estimate with the CDF of the observed daily precipitation distribution.The results obtained are then similar to those of the literature, which also attests to the fact that the QEM is recognised as a powerful method for reducing the systematic bias of precipitation estimates from regional climate models. Therefore, it has consistently demonstrated the best skill (Yang et al. 2016; Themeßl et al. 2011, 2012; Alharbi 2019). However, against all expectations, the validation of the monthly time step gave unexpected results since EQM performs poorly in front of TSV. (Oruc et al. 2022) in his analysis also found that the Delta (DT) method slightly outperformed the other bias correction techniques (EQM and GQM) for the monthly timescale. Also contrary to the results of our studies, sometimes the uncorrected SPDs can outperform the bias-corrected SPEs in the reproduction of rainfall depths. This means that there is a deterioration of some statistics after the bias correction. A similar result is shown in (Omodi 2017; Teng et al 2015) for southern Murray where bias correction gave poor results. Additional errors can therefore be introduced by some bias correction techniques, indicating how inefficient bias correction methods can be.

- Merging of SPDs
  Merging take advantage of the benefits of remote sensing and the rain gauge to achieve better results, compared to using them individually. This would mean that the technique is considered advantageous when it provides better quality outputs than both data sets (i.e. in terms of spatial and temporal, accuracy and event occurrences). In this study,

the merging of satellite precipitation products with precipitation measurements gives satisfactory results as confirmed by Duque-Gardeazábal et al. (2018) and Bhuiyan et al. (2019). All the approaches presented very close scores and none of them had lower scores than the original data. RK and MFB belong to the interpolation and bias correction category of merging methods respectively. Ochoa-Rodriguez et al. (2019) and Qiu et al. (2020) ranked the categories of merging methods from the best to the worst performing as follows: integration category; interpolation category and bias correction category. The results of this study which ranks RK above the others are confirmed by the performances ranking. On the other hand, Lakew et al.(2020) suggest that it is then not necessary to merge the MSWEP data set with the sparsely located rain gauges data over on the Nile. A simple bias correction is sufficient as the merged data performed worse than the corrected ones.

Conclusion and Perspectives

Conclusion

This study aimed to improve the gridded precipitation data over Burkina Faso. To achieve this, an evaluation was first conducted to identify the most suitable SPDs as an alternative to the in situ data from rain gauges. The validation by climate zone showed that tamsat v3.1 is the best for reproducing station rainfall data for all zones at the daily scale, followed by rfev2. But for the monthly scale analysis, the Chirps V2.0 dataset showed the best estimates for the Sahelian and Sudano-Sahelian zones ahead of TRMM-3B42. Over the Sudanian zone, Persisian-CDR best reproduced the rainfall data from the rain gauges. The GPCP performed worst in all validation tests performed at daily time step, while Arc2 and Tamsat were among the worst performers at monthly time step. Two bias correction schemes have been applied to remove bias from the TAMSATV3.1 and CHIRPS V2.0 estimates. The empirical quantile mapping and the space-time variant were used individually to correct these datasets. Both showed improved statistics compared to the original data when assessing the corrected datasets. However, EQM shows a significant improvement compared to TSV at the daily scale while TSV was more appropriate for the monthly scale. The four Merging techniques RK-Spheremap, RK-Shepard, MFB-Spheremap, and MFB-Shepard have been proven to increase accuracy, primarily by reducing root mean square error (RMSE), mean error (ME), the bias, and increasing the correlation. The best blending method in descending order in this study is RK-Spheremap, MFB-Spheremap, RK-Shepard, MFB-Shepard. This order is the same for both daily and monthly time steps. After the bias correction and merging steps, the following improvements were observed: An improvement in the correlation of the daily data of 85.2%, the Bias of 12.4% and the RMSE of 95.6%. For the monthly data, the correlation coefficients are improved by 8.4%, the bias by 2.3% and the RMSE by 99.9%. Based on the results, the proposed approach that combines the three steps (SPD assessment, SPD bias correction and datasets merging) has therefore the potential to significantly improve the quality of precipitation estimates by satellite for operational

applications. It could be a good alternative to help forecasters, agencies, organizations and other entities in their work with the population and research (studies of drought, flooding, cropping calendars, etc). Verification of the hypothesis of this research:

- Based on the results of the validations performed, the first assumption stating that as the time step of the evaluation increases, the performance of the SPDs improves is accepted. Indeed, satellite estimates at monthly time scale are more accurate than the daily time scale.
- The second assumption is that the bias-corrected data set has a significantly reduced systematic bias with MQE compared to TSV. This hypothesis is half-tested as it is accepted for the daily time step but rejected for the monthly time scale.
- The third assumption is the following: The reliability of the bias-corrected data sets is improved by merging them with the rain gauge observations. It is accepted for all time scales and all methods, even for the worst ones.

Perspectives

In a future study, the proposed assessment could be performed to assess the accuracy of satellite products in capturing extreme precipitation events. In general, all satellite products exhibit many errors in extreme precipitation estimates, as mentioned by Jiang et al. (2019). In response to climate change, improving the accuracy of SPDs on the quantity and frequency of extreme events, especially in extreme precipitation, is key to anticipatory strategies such as flood forecasting and drought monitoring. On the other and, there is a need to conduct study on the impact of rain gauge density on Merging performance in Burkina Faso. The maintenance of meteorological stations is very expensive and this survey could guide the minimum number of stations to be kept and seriously maintained in order to obtain quality data when it comes to merging these rain gauges with satellite data. As a long term perspective, it is planned to carry out similar study on temperature because Burkina Faso has only 10 reliable temperature measurement points. Although the temperature is a continuous variable, this network is insufficient. A similar study would avail temperature datasets for decision making and heat wave monotoring in the country.

Bibliography

Alharbi, R. (2019). *Bias Adjustment of Satellite-Based Precipitation Estimation Using Limited Gauge Measurements and Its Implementation on Hydrologic Modeling*. Ph. D. thesis, UC Irvine.

Ali, A., T. Lebel, and A. Amani (2008). Signification et usage de l'indice pluviométrique au sahel. *Science et changements planétaires/Sécheresse 19*(4), 227–235.

Ashouri, H., K.-L. Hsu, S. Sorooshian, D. K. Braithwaite, K. R. Knapp, L. D. Cecil, B. R. Nelson, and O. P. Prat (2015). Persiann-cdr: Daily precipitation climate data record from multisatellite observations for hydrological and climate studies. *Bulletin of the American Meteorological Society 96*(1), 69–83.

Atiah, W. A., L. K. Amekudzi, J. N. A. Aryee, K. Preko, and S. K. Danuor (2020). Validation of satellite and merged rainfall data over ghana, west africa. *Atmosphere 11*(8), 859.

Bayissa, Y., T. Tadesse, G. Demisse, and A. Shiferaw (2017). Evaluation of satellite-based rainfall estimates and application to monitor meteorological drought for the upper blue nile basin, ethiopia. *Remote Sensing 9*(7), 669.

Beck, H. E., A. I. Van Dijk, V. Levizzani, J. Schellekens, D. G. Miralles, B. Martens, and A. De Roo (2017). Mswep: 3-hourly 0.25 global gridded precipitation (1979–2015) by merging gauge, satellite, and reanalysis data. *Hydrology and Earth System Sciences 21*(1), 589–615.

Becker, A., P. Finger, A. Meyer-Christoffer, B. Rudolf, K. Schamm, U. Schneider, and M. Ziese (2013). A description of the global land-surface precipitation data products of the global precipitation climatology centre with sample applications including centennial (trend) analysis from 1901–present. *Earth System Science Data 5*(1), 71–99.

Bhuiyan, M. A., E. I. Nikolopoulos, and E. N. Anagnostou (2019). Machine learning–based blending of satellite and reanalysis precipitation datasets: A multiregional tropical complex terrain evaluation. *Journal of Hydrometeorology 20*(11), 2147–2161.

Capacci, D. and F. Porcu (2009). Evaluation of a satellite multispectral vis–ir daytime statistical rain-rate classifier and comparison with passive microwave rainfall estimates. *Journal of applied meteorology and climatology 48*(2), 284–300.

Chappell, A., L. J. Renzullo, T. H. Raupach, and M. Haylock (2013). Evaluating geostatistical methods of blending satellite and gauge data to estimate near real-time daily rainfall for australia. *Journal of hydrology 493*, 105–114.

Chen, J., F. P. Brissette, D. Chaumont, and M. Braun (2013). Finding appropriate bias correction methods in downscaling precipitation for hydrologic impact studies over north america. *Water Resources Research 49*(7), 4187–4205.

Chen, M., P. Xie, J. E. Janowiak, and P. A. Arkin (2002). Global land precipitation: A 50-yr monthly analysis based on gauge observations. *Journal of Hydrometeorology 3*(3), 249–266.

Conti, F. L., K.-L. Hsu, L. V. Noto, and S. Sorooshian (2014). Evaluation and comparison of satellite precipitation estimates with reference to a local area in the mediterranean sea. *Atmospheric Research 138*, 189–204.

De Vera, A., P. Alfaro, and R. Terra (2021). Operational implementation of satellite-rain gauge data merging for hydrological modeling. *Water 13*(4), 533.

Dembélé, M. and S. J. Zwart (2016). Evaluation and comparison of satellite-based rainfall products in burkina faso, west africa. *International Journal of Remote Sensing 37*(17), 3995–4014.

Dinku, T., S. Chidzambwa, P. Ceccato, S. Connor, and C. Ropelewski (2008). Validation of high-resolution satellite rainfall products over complex terrain. *International Journal of Remote Sensing 29*(14), 4097–4110.

Dinku, T., R. Cousin, J. del Corral, and P. Ceccato (2016). The enacts approach: Transforming climate services in africa, one country at a time a world policy paper.

Dinku, T., F. Ruiz, S. J. Connor, and P. Ceccato (2010). Validation and intercomparison of satellite rainfall estimates over colombia. *Journal of Applied Meteorology and Climatology 49*(5), 1004–1014.

Duque-Gardeazábal, N., D. Zamora, and E. Rodríguez (2018). Analysis of the kernel bandwidth influence in the double smoothing merging algorithm to improve rainfall fields in poorly gauged basins. In *HIC 2018: 13th Int. Conf. on Hydroinformatics*, Volume 3, pp. 635–642.

Ebert, E. E., J. E. Janowiak, and C. Kidd (2007). Comparison of near-real-time precipitation estimates from satellite observations and numerical models. *Bulletin of the American Meteorological Society 88*(1), 47–64.

Faso, B. (2007). Programme d'action national d'adaptation a la variabilité et aux changements climatiques (pana du burkina faso). *Minitsère de l'Environnement et du Cadre de Vie: Burkina Faso Tech. rep*.

Funk, C., P. Peterson, M. Landsfeld, D. Pedreros, J. Verdin, S. Shukla, G. Husak, J. Rowland, L. Harrison, A. Hoell, et al. (2015). The climate hazards infrared precipitation with stations—a new environmental record for monitoring extremes. *Scientific data 2*(1), 1–21.

Gebremichael, M., M. M. Bitew, F. A. Hirpa, and G. N. Tesfay (2014). Accuracy of satellite rainfall estimates in the b lue n ile b asin: L owland plain versus highland mountain. *Water Resources Research 50*(11), 8775–8790.

GIARNO, G., H. M. PROMONO, S. SLAMET, and H. SIGIT (2020). Bias correction of radar and satellite rainfall estimates and increasing its accuracy using modified merging. *Mausam 71*(3), 377–390.

Giarno, M. P. H., S. Suprayogi, S. Herumurti, et al. (2018). Modified mean field bias and local bias for improvement bias corrected satellite rainfall estimates. *Mausam 69*(4), 543–552.

Goovaerts, P. (1999). Geostatistics in soil science: state-of-the-art and perspectives.

Goovaerts, P. et al. (1997). *Geostatistics for natural resources evaluation*. Oxford University Press on Demand.

Goshime, D. (2020). *Integration of satellite and ground-based rainfall data for water resources assessment in Central Rift Valley Lakes Basin, Ethiopia*. Ph. D. thesis, CY Cergy Paris Université.

Gosset, M., J. Viarre, G. Quantin, and M. Alcoba (2013). Evaluation of several rainfall products used for hydrological applications over west africa using two high-resolution gauge networks. *Quarterly Journal of the Royal Meteorological Society 139*(673), 923–940.

Goudenhoofdt, E. and L. Delobbe (2009). Evaluation of radar-gauge merging methods for quantitative precipitation estimates. *Hydrology and Earth System Sciences 13*(2), 195–203.

Groisman, P. Y. and D. R. Legates (1995). Documenting and detecting long-term precipitation trends: where we are and what should be done. *Climatic change 31*(2), 601–622.

Gumindoga, W., T. Rientjes, A. Haile, H. Makurira, and P. Reggiani (2016). Bias correction schemes for cmorph satellite rainfall estimates in the zambezi river basin. *Hydrology and Earth System Sciences Discussions*, 1–36.

Gumindoga, W., T. H. Rientjes, A. T. Haile, H. Makurira, and P. Reggiani (2019). Performance of bias-correction schemes for cmorph rainfall estimates in the zambezi river basin. *Hydrology and earth system sciences 23*(7), 2915–2938.

Habib, E., A. T. Haile, N. Sazib, Y. Zhang, and T. Rientjes (2014). Effect of bias correction of satellite-rainfall estimates on runoff simulations at the source of the upper blue nile. *Remote Sensing 6*(7), 6688–6708.

Harris, I., P. D. Jones, T. J. Osborn, and D. H. Lister (2014). Updated high-resolution grids of monthly climatic observations–the cru ts3. 10 dataset. *International journal of climatology 34*(3), 623–642.

Hengl, T., G. B. Heuvelink, and D. G. Rossiter (2007). About regression-kriging: From equations to case studies. *Computers & geosciences 33*(10), 1301–1315.

Hengl, T., G. B. Heuvelink, and A. Stein (2004). A generic framework for spatial prediction of soil variables based on regression-kriging. *Geoderma 120*(1-2), 75–93.

Huffman, G. J., R. F. Adler, D. T. Bolvin, and E. J. Nelkin (2010). The trmm multi-satellite precipitation analysis (tmpa). In *Satellite rainfall applications for surface hydrology*, pp. 3–22. Springer.

Huffman, G. J., D. T. Bolvin, D. Braithwaite, K. Hsu, R. Joyce, P. Xie, and S.-H. Yoo (2015). Nasa global precipitation measurement (gpm) integrated multi-satellite retrievals for gpm (imerg). *Algorithm Theoretical Basis Document (ATBD) Version 4*, 26.

Jakob Themeßl, M., A. Gobiet, and A. Leuprecht (2011). Empirical-statistical downscaling and error correction of daily precipitation from regional climate models. *International Journal of Climatology 31*(10), 1530–1544.

Javanmard, S., A. Yatagai, M. Nodzu, J. BodaghJamali, and H. Kawamoto (2010). Comparing high-resolution gridded precipitation data with satellite rainfall estimates of trmm_3b42 over iran. *Advances in Geosciences 25*, 119–125.

Jiang, D. and K. Wang (2019). The role of satellite-based remote sensing in improving simulated streamflow: A review. *Water 11*(8), 1615.

Jobard, I., F. Chopin, J. C. Bergès, and R. Roca (2011). An intercomparison of 10-day satellite precipitation products during west african monsoon. *International Journal of Remote Sensing 32*(9), 2353–2376.

Joyce, R. J., J. E. Janowiak, P. A. Arkin, and P. Xie (2004). Cmorph: A method that produces global precipitation estimates from passive microwave and infrared data at high spatial and temporal resolution. *Journal of hydrometeorology 5*(3), 487–503.

Katsanos, D., A. Retalis, and S. Michaelides (2016). Validation of a high-resolution precipitation database (chirps) over cyprus for a 30-year period. *Atmospheric Research 169*, 459–464.

Kidd, C., A. Becker, G. J. Huffman, C. L. Muller, P. Joe, G. Skofronick-Jackson, and D. B. Kirschbaum (2017). So, how much of the earth's surface is covered by rain gauges? *Bulletin of the American Meteorological Society 98*(1), 69–78.

Kim, D., H.-H. Kwon, S.-O. Lee, and S. Kim (2016). Regionalization of the modified bartlett–lewis rectangular pulse stochastic rainfall model across the korean peninsula. *Journal of Hydro-environment Research 11*, 123–137.

Lafon, T., S. Dadson, G. Buys, and C. Prudhomme (2013). Bias correction of daily precipitation simulated by a regional climate model: a comparison of methods. *International Journal of Climatology 33*(6), 1367–1381.

Lakew, H. B., S. A. Moges, and D. H. Asfaw (2020). Hydrological performance evaluation of multiple satellite precipitation products in the upper blue nile basin, ethiopia. *Journal of Hydrology: Regional Studies 27*, 100664.

Leander, R. and T. A. Buishand (2007). Resampling of regional climate model output for the simulation of extreme river flows. *Journal of Hydrology 332*(3-4), 487–496.

Lebel, T., A. Diedhiou, and H. Laurent (2003). Seasonal cycle and interannual variability of the sahelian rainfall at hydrological scales. *Journal of Geophysical Research: Atmospheres 108*(D8).

Lenderink, G., A. Buishand, and W. Van Deursen (2007). Estimates of future discharges of the river rhine using two scenario methodologies: direct versus delta approach. *Hydrology and Earth System Sciences 11*(3), 1145–1159.

Lensky, I. M. and V. Levizzani (2008). Estimation of precipitation from space-based platforms. In *Precipitation: Advances in measurement, estimation and prediction*, pp. 195–217. Springer.

Levizzani, V., J. Schmetz, H. Lutz, J. Kerkmann, P. Alberoni, and M. Cervino (2001). Precipitation estimations from geostationary orbit and prospects for meteosat second generation. *Meteorological Applications 8*(1), 23–41.

Maidment, R. I., D. Grimes, R. P. Allan, E. Tarnavsky, M. Stringer, T. Hewison, R. Roebeling, and E. Black (2014). The 30 year tamsat african rainfall climatology and time series (tarcat) data set. *Journal of Geophysical Research: Atmospheres 119*(18), 10–619.

Malvić, T., J. Ivšinović, J. Velić, J. Sremac, and U. Barudžija (2020). Application of the modified shepard's method (msm): A case study with the interpolation of neogene reservoir variables in northern croatia. *Stats 3*(1), 68–83.

Matsuura, K. and C. J. Willmott (2009). Terrestrial precipitation: 1900–2008 gridded monthly time series. *Center for Climatic Research Department of Geography Center for Climatic Research, University of Delaware*.

McKee, J. L. (2015). Evaluation of gauge-radar merging methods for quantitative precipitation estimation in hydrology: A case study in the upper thames river basin.

Meng, J., L. Li, Z. Hao, J. Wang, and Q. Shao (2014). Suitability of trmm satellite rainfall in driving a distributed hydrological model in the source region of yellow river. *Journal of Hydrology 509*, 320–332.

Menne, M. J., I. Durre, R. S. Vose, B. E. Gleason, and T. G. Houston (2012). An overview of the global historical climatology network-daily database. *Journal of atmospheric and oceanic technology 29*(7), 897–910.

Nerini, D., Z. Zulkafli, L.-P. Wang, C. Onof, W. Buytaert, W. Lavado-Casimiro, and J.-L. Guyot (2015). A comparative analysis of trmm–rain gauge data merging techniques at the daily time scale for distributed rainfall–runoff modeling applications. *Journal of Hydrometeorology 16*(5), 2153–2168.

New, M., M. Todd, M. Hulme, and P. Jones (2001). Precipitation measurements and trends in the twentieth century. *International Journal of Climatology: A Journal of the Royal Meteorological Society 21*(15), 1889–1922.

Nicholson, S. E., B. Some, J. McCollum, E. Nelkin, D. Klotter, Y. Berte, B. Diallo, I. Gaye, G. Kpabeba, O. Ndiaye, et al. (2003). Validation of trmm and other rainfall estimates with a high-density gauge dataset for west africa. part i: Validation of gpcc rainfall product and pre-trmm satellite and blended products. *Journal of Applied Meteorology 42*(10), 1337–1354.

Novella, N. S. and W. M. Thiaw (2013). African rainfall climatology version 2 for famine early warning systems. *Journal of Applied meteorology and Climatology 52*(3), 588–606.

Ochoa-Rodriguez, S., L. Wang, A. Bailey, A. Schellart, P. Willems, and C. Onof (2015). Evaluation of radar-rain gauge merging methods for urban hydrological applications: Relative performance and impact of gauge density. *UrbanRain15 Proceedings "Rainfall in Urban and Natural Systems"*.

Ochoa-Rodriguez, S., L.-P. Wang, P. Willems, and C. Onof (2019). A review of radar-rain gauge data merging methods and their potential for urban hydrological applications. *Water Resources Research 55*(8), 6356–6391.

Odeh, I. O., A. McBratney, and D. Chittleborough (1995). Further results on prediction of soil properties from terrain attributes: heterotopic cokriging and regression-kriging. *Geoderma 67*(3-4), 215–226.

Omondi, C. K. (2017). Assessment of bias corrected satellite rainfall products for streamflow simulation: a topmodel application in the kabompo river basin, zambia. Master's thesis, University of Twente.

Organization, W. M. (2008). Guide to hydrological practices. volume i: Hydrology—from measurement to hydrological information. *WMO-No. 168*.

Oruc, S. (2022). Performance of bias corrected monthly cmip6 climate projections with different reference period data in turkey. *Acta Geophysica 70*(2), 777–789.

Pfeifroth, U., R. Mueller, and B. Ahrens (2013). Evaluation of satellite-based and reanalysis precipitation data in the tropical pacific. *Journal of Applied Meteorology and Climatology 52*(3), 634–644.

Pham Gia, T., M. Kappas, C. Van Huynh, and L. Hoang Khanh Nguyen (2019). Application of ordinary kriging and regression kriging method for soil properties mapping in hilly region of central vietnam. *ISPRS International Journal of Geo-Information 8*(3), 147.

Qin, Y., Z. Chen, Y. Shen, S. Zhang, and R. Shi (2014). Evaluation of satellite rainfall estimates over the chinese mainland. *Remote Sensing 6*(11), 11649–11672.

Qiu, Q., J. Liu, J. Tian, Y. Jiao, C. Li, W. Wang, and F. Yu (2020). Evaluation of the radar qpe and rain gauge data merging methods in northern china. *Remote Sensing 12*(3), 363.

Roudier, P., B. Sultan, P. Quirion, and A. Berg (2011). The impact of future climate change on west african crop yields: what does the recent literature say? *Global environmental change 21*(3), 1073–1083.

Sadeghi, M., A. A. Asanjan, M. Faridzad, P. Nguyen, K. Hsu, S. Sorooshian, and D. Braithwaite (2019). Persiann-cnn: Precipitation estimation from remotely sensed information using artificial neural networks–convolutional neural networks. *Journal of Hydrometeorology 20*(12), 2273–2289.

Schamm, K., M. Ziese, A. Becker, P. Finger, A. Meyer-Christoffer, U. Schneider, M. Schröder, and P. Stender (2014). Global gridded precipitation over land: A description of the new gpcc first guess daily product. *Earth System Science Data 6*(1), 49–60.

Schmidli, J., C. Frei, and P. L. Vidale (2006). Downscaling from gcm precipitation: a benchmark for dynamical and statistical downscaling methods. *International Journal of Climatology: A Journal of the Royal Meteorological Society 26*(5), 679–689.

Sevruk, B. (1997). Regional dependency of precipitation-altitude relationship in the swiss alps. In *Climatic change at high elevation sites*, pp. 123–137. Springer.

Shrestha, N. K., F. M. Qamer, D. Pedreros, M. Murthy, S. M. Wahid, and M. Shrestha (2017). Evaluating the accuracy of climate hazard group (chg) satellite rainfall estimates for precipitation based drought monitoring in koshi basin, nepal.

Simbahan, G. C., A. Dobermann, P. Goovaerts, J. Ping, and M. L. Haddix (2006). Fine-resolution mapping of soil organic carbon based on multivariate secondary data. *Geoderma 132*(3-4), 471–489.

Smith, T. M., P. A. Arkin, J. J. Bates, and G. J. Huffman (2006). Estimating bias of satellite-based precipitation estimates. *Journal of Hydrometeorology 7*(5), 841–856.

Soo, E. Z. X., W. Z. W. Jaafar, S. H. Lai, F. Othman, A. Elshafie, T. Islam, P. Srivastava, and H. S. O. Hadi (2020). Evaluation of bias-adjusted satellite precipitation estimations for extreme flood events in langat river basin, malaysia. *Hydrology Research 51*(1), 105–126.

Stisen, S., A. Højberg, L. Troldborg, J. Refsgaard, B. Christensen, M. Olsen, and H. Henriksen (2012). On the importance of appropriate precipitation gauge catch correction for hydrological modelling at mid to high latitudes. *Hydrology and Earth System Sciences 16*(11), 4157–4176.

Strangeways, I. et al. (2010). A history of rain gauges. *Weather 65*(5), 133–138.

Sumfleth, K. and R. Duttmann (2008). Prediction of soil property distribution in paddy soil landscapes using terrain data and satellite information as indicators. *Ecological indicators 8*(5), 485–501.

Sun, Q., C. Miao, Q. Duan, H. Ashouri, S. Sorooshian, and K.-L. Hsu (2018). A review of global precipitation data sets: Data sources, estimation, and intercomparisons. *Reviews of Geophysics 56*(1), 79–107.

Tang, L., Y. Tian, F. Yan, and E. Habib (2015). An improved procedure for the validation of satellite-based precipitation estimates. *Atmospheric Research 163*, 61–73.

Taylor, K. E. (2001). Summarizing multiple aspects of model performance in a single diagram. *Journal of Geophysical Research: Atmospheres 106*(D7), 7183–7192.

Tazen, F., A. Diarra, R. F. Kabore, B. Ibrahim, M. Bologo/Traoré, K. Traoré, and H. Karambiri (2019). Trends in flood events and their relationship to extreme rainfall in an urban area of sahelian west africa: The case study of ouagadougou, burkina faso. *Journal of Flood Risk Management 12*, e12507.

Teng, H., Z. Ma, A. Chappell, Z. Shi, Z. Liang, and W. Yu (2017). Improving rainfall erosivity estimates using merged trmm and gauge data. *Remote Sensing 9*(11), 1134.

Teutschbein, C. and J. Seibert (2012). Bias correction of regional climate model simulations for hydrological climate-change impact studies: Review and evaluation of different methods. *Journal of hydrology 456*, 12–29.

Themeßl, M. J., A. Gobiet, and G. Heinrich (2012). Empirical-statistical downscaling and error correction of regional climate models and its impact on the climate change signal. *Climatic Change 112*(2), 449–468.

Toté, C., D. Patricio, H. Boogaard, R. Van der Wijngaart, E. Tarnavsky, and C. Funk (2015). Evaluation of satellite rainfall estimates for drought and flood monitoring in mozambique. *Remote Sensing 7*(2), 1758–1776.

Tramblay, Y., V. Thiemig, A. Dezetter, and L. Hanich (2016). Evaluation of satellite-based rainfall products for hydrological modelling in morocco. *Hydrological Sciences Journal 61*(14), 2509–2519.

Verdin, A., C. Funk, B. Rajagopalan, and W. Kleiber (2016). Kriging and local polynomial methods for blending satellite-derived and gauge precipitation estimates to support hydrologic early warning systems. *IEEE Transactions on Geoscience and Remote Sensing 54*(5), 2552–2562.

Verdin, A. P. (2013). *Statistical methods for blending satellite and ground observations to improve high-resolution precipitation estimates*. Ph. D. thesis, University of Colorado at Boulder.

Wang, L.-P., S. Ochoa-Rodríguez, N. E. Simões, C. Onof, and Č. Maksimović (2013). Radar–raingauge data combination techniques: a revision and analysis of their suitability for urban hydrology. *Water science and technology 68*(4), 737–747.

Wilks, D. S. (2011). *Statistical methods in the atmospheric sciences*, Volume 100. Academic press.

Xie, P., M. Chen, and W. Shi (2010). Cpc unified gauge-based analysis of global daily precipitation. In *Preprints, 24th Conf. on Hydrology, Atlanta, GA, Amer. Meteor. Soc*, Volume 2.

Yang, Z., K. Hsu, S. Sorooshian, X. Xu, D. Braithwaite, and K. M. Verbist (2016). Bias adjustment of satellite-based precipitation estimation using gauge observations: A case study in chile. *Journal of Geophysical Research: Atmospheres 121*(8), 3790–3806.

Appendix

Appendix 1: Scatter plots of daily data

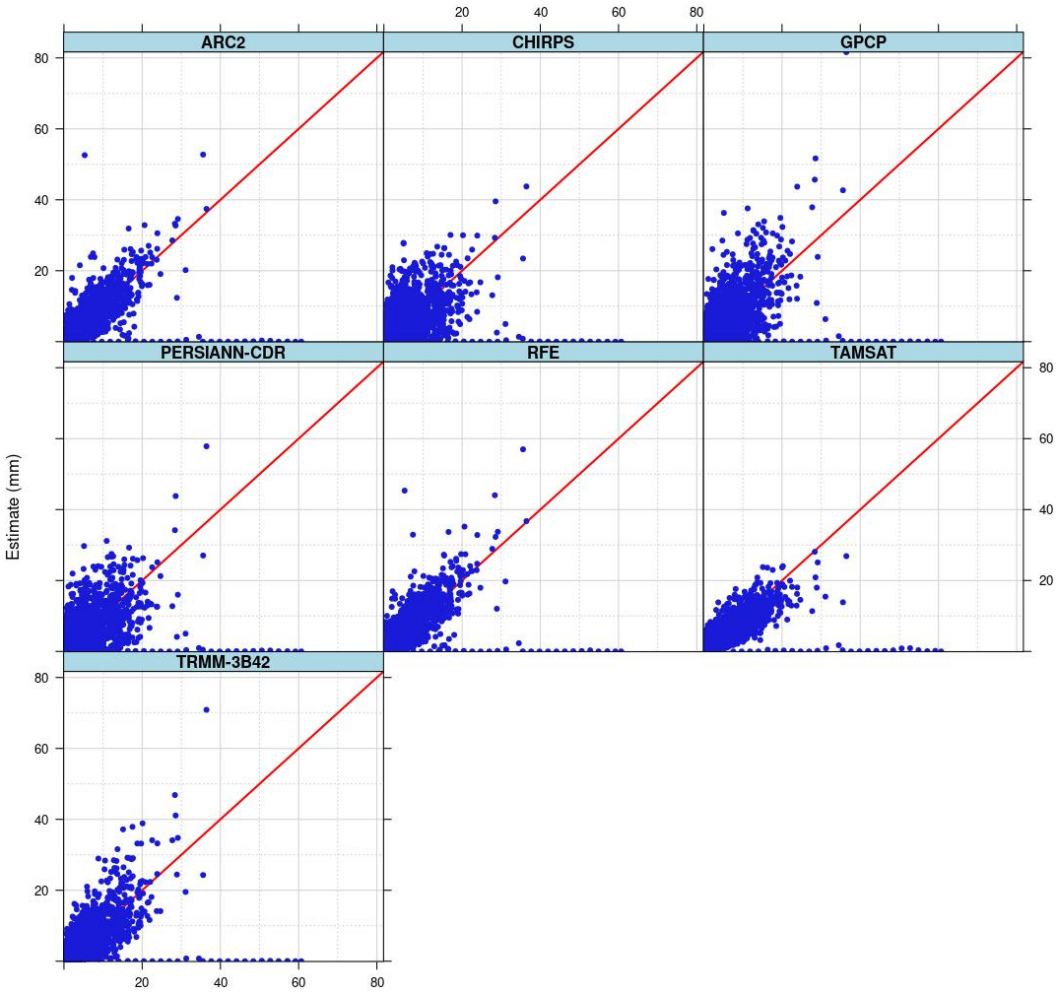

Figure 3.14: Scatter plots of daily data between the rain gauge observations and the satellites precipitation datasets

Appendix 2: Scatter plots of monthly data

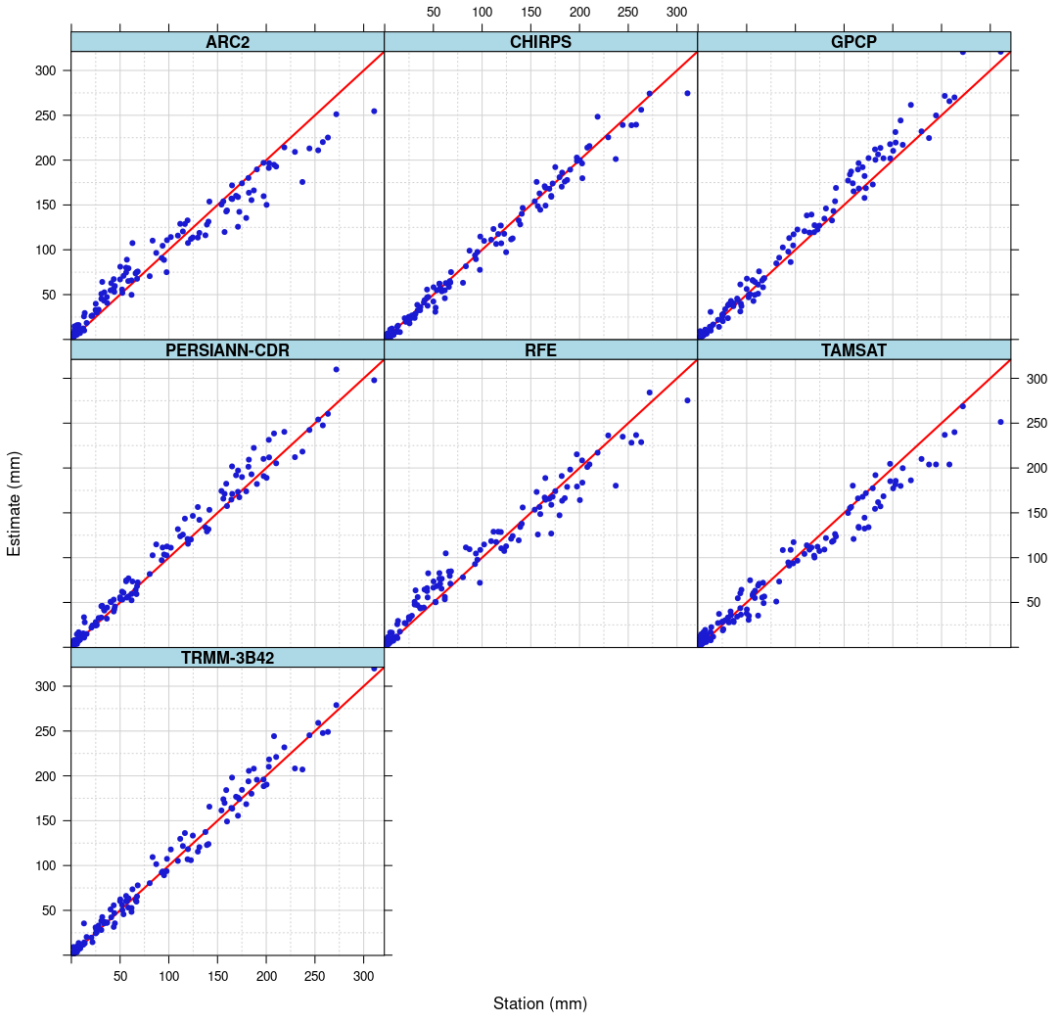

Figure 3.15: Scatter plots of monthly data between the rain gauge observations and the satellites precipitation datasets

Appendix 3: list of weather stations

Table 3.9: List of stations involved in this study, their coordinates and data availability on the study period (2001-2014)

ID	Stations	Longitude	Latitude	Number of observations	Data avaibility(
1	Ouagadougou aero	-1.512393	12.356415	5114	100
2	Ouarkoye	-3.666936	12.095299	5114	99.37
3	Baraboule	-1.851861	14.207478	5114	99.98
4	Aribinda	-0.867899	14.227154	5114	98.81
5	Gorgadji	-0.517171	14.034129	5114	98.83
6	Gorom Gorom	-0.23464	14.443475	5114	97.54
7	Dori	-0.036463	14.033881	5114	100
8	Di Sourou	-3.405409	13.164027	5114	98.18
9	Kassoum	-3.301386	13.07371	5114	98.79
10	Toeni	-3.183169	13.439303	5114	95.81
11	Tougan	-3.071034	13.065523	5114	98.18
12	Kiembara	-2.726192	13.240201	5114	99.41
13	Ouahigouya	-2.416512	13.565299	5114	100
14	Gourcy	-2.354984	13.196727	5114	99.94
15	Titao	-2.072084	13.767296	5114	99.98
16	Seguenega	-1.966787	13.437844	5114	98.81
17	Pobe Mengao	-1.765525	13.90174	5114	99.39
18	Tema Bokin	-1.803654	13.002054	5114	100
19	Bourzanga	-1.55029	13.673307	5114	97.03
20	Barsalogho	-1.057686	13.41711	5114	99.98
21	Tougouri	-0.525729	13.312797	5114	98.81
22	Dakiri	-0.255089	13.291822	5114	100
23	Sebba	0.525059	13.44342	5114	97.03
24	Tansila	-4.388455	12.418673	5114	100
25	Solenzo	-4.083315	12.179734	5114	98.79
26	Nouna	-3.85968	12.731276	5114	99.98
27	Dedougou	-3.481938	12.463666	5114	100
28	Sourou Gassan	-3.202195	12.821941	5114	95.21
29	Safane	-3.229567	12.129048	5114	97.03
30	Toma	-2.893941	12.760481	5114	98.81
31	Tiogo	-2.689818	12.178328	5114	97.56
32	Reo Agri	-2.458194	12.308788	5114	98.22
33	Yako	-2.264181	12.958272	5114	95.01
34	Nanoro	-2.194683	12.686784	5114	99.96
35	Saria	-2.157301	12.268978	5114	97.52
36	Kindi	-2.040228	12.435306	5114	99.39
37	Bousse	-1.897604	12.660495	5114	98.71
38	Kokologho	-1.882237	12.194405	5114	98.18
39	Tanghin Dassouri	-1.717807	12.269062	5114	99.39
40	Kamboince	-1.548466	12.456776	5114	98.79

ID	Stations	Longitude	Latitude	Number of observations	Data avaibility(
41	Mane	-1.346356	12.984888	5114	97.61
42	Kombissiri	-1.332234	12.053305	5114	95.78
43	Guilongou	-1.307974	12.613202	5114	96.99
44	Korsimoro	-1.069292	12.828292	5114	97.63
45	Mogtedo	-0.834057	12.285242	5114	98.77
46	Zorgho	-0.609076	12.246673	5114	99.98
47	Boulsa	-0.568152	12.663798	5114	96.44
48	Koupela	-0.353174	12.182407	5114	99.96
49	Bogande	-0.160714	12.979046	5114	100
50	Piela	-0.132112	12.70382	5114	98.22
51	Bilanga	-0.027002	12.545484	5114	98.22
52	Fada Ngourma	0.364598	12.045793	5114	100
53	Yamba	0.33621	12.295897	5114	98.81
54	Gayeri	0.488548	12.651833	5114	100
55	Farako Ba	-4.332049	11.094406	5114	98.75
56	Bobo Dioulasso	-4.322019	11.162578	5114	100
57	Bondoukuy	-3.750286	11.868359	5114	98.79
58	Koumbia	-3.6961	11.236369	5114	99.96
59	Bereba	-3.680498	11.621707	5114	96.54
60	Hounde	-3.521113	11.486433	5114	99.39
61	Wona	-3.42946	11.971107	5114	97.56
62	Dano	-3.066343	11.147352	5114	97.57
63	Boromo	-2.929275	11.744512	5114	100
64	Boura	-2.506202	11.039217	5114	99.39
65	Thiou Koudougou	-2.197553	11.951494	5114	99.39
66	Betare	-1.375108	11.433402	5114	98.2
67	Po	-1.146324	11.180598	5114	100
68	Manga	-1.071816	11.662119	5114	97.11
69	Niaogho	-0.771272	11.773527	5114	96.97
70	Garango	-0.547514	11.804819	5114	99.39
71	Ouargaye	0.057861	11.504821	5114	98.81
72	Pama	0.704708	11.247395	5114	100
73	Mahadaga	1.778134	11.73859	5114	96.44
74	Baguera	-5.424457	10.531927	5114	99.39
75	Loumana	-5.346318	10.578826	5114	99.98
76	Sindou	-5.163608	10.660583	5114	99.39
77	Soubakaniedougou	-5.002553	10.474577	5114	100
78	Orodara	-4.926081	10.97948	5114	96.97
79	Niangoloko	-4.908429	10.271126	5114	99.9
80	Banfora Agri	-4.763896	10.638829	5114	98.79
81	Sideradougou	-4.252861	10.67638	5114	99.98

ID	Stations	Longitude	Latitude	Number of observations	Data avaibility(
82	Ouo	-3.846168	10.398932	5114	97.59
83	Kampti	-3.458564	10.142647	5114	97.01
84	Gaoua	-3.166372	10.385551	5114	100
85	Batie	-2.918969	9.880645	5114	95.81
86	Leri	-3.384891	12.763163	5114	100
87	Botou	2.049382	12.664599	5114	97.61
88	Ndorola	-4.725886	11.782906	5114	97.63
89	Kouka	-4.337164	11.905404	5114	95.87
90	Vallee DuKou	-4.233336	11.132045	5114	100
91	Fara	-2.762335	11.520394	5114	99.43
92	Beregadougou	-4.727879	10.747085	5114	100
93	Ouangolodougou	-4.805891	10.069083	5114	99.98
94	Bitou	-0.29983	11.25929	5114	95.19
95	Nobere	-1.201876	11.559971	5114	100
96	Bingo	-1.834	12.30855	5114	96.3
97	Namoungou	0.658177	12.040254	5114	95.29

Table of Contents

Dedication i
Acknowledgments ii
Abstract iii
Acronyms and Abbreviations v
Acronyms and Abbreviations vi
List of Tables vii
List of Figures viii

Chapter 1: Literature review **6**
1.1 Precipitation observation systems 6
1.1.1 Rain gauge measurements 6
1.1.2 Uncertainties in rain gauge measurements 7
1.1.3 Meteorological Radars 8
1.1.4 Satellite precipitation estimates 8
1.1.4.1 Satellite measurement principles 9
The Visible and Infrared 10
Passive Microwave 10
Multi-Sensor Technique 11
1.2 Evaluation of SPDs 12
1.2.1 Summary of the previous studies on the evaluations of SPDs 12
1.2.2 Verification statistics for precipitation satellite datasets 12
1.2.3 Some verification results of precipitation satellite datasets 12
1.3 Bias Correction of SPDs 13
1.3.1 Satellites -Rain Gauge Bias Correction Methods 13
1.3.2 Relative Advantages and Disadvantages of the most common Correction Methods 14
1.3.3 Intercomparison of bias Adjustment Methods 14

1.4 Merging of SPDs and rain gauges data . . . 17
1.4.1 Satellites -Rain Gauge Blending Methods . . . 17
1.4.2 Relative Advantages and Disadvantages of some blending Methods . . . 17
1.4.3 Intercomparison of Merging Methods . . . 18
1.5 Summary of gaps based on literature review . . . 21

Chapter 2: Methodology **22**
2.1 Study Area . . . 22
2.1.1 Geographic location . . . 22
2.1.2 Climatology . . . 23
2.2 Data . . . 24
2.2.1 Rain Gauges data . . . 24
2.2.2 Satellite Precipitation datasets . . . 25
2.3 Tools . . . 29
2.4 Methods . . . 31
2.4.1 Validation of Satellite precipitation datasets . . . 32
2.4.1.1 Validation process . . . 32
2.4.1.2 Validation Statistics . . . 32
2.4.2 Bias adjustment . . . 36
2.4.2.1 Empirical Quantile mapping . . . 36
2.4.2.2 Time and space-variant bias correction . . . 37
2.4.3 Merging Approach . . . 38
2.4.3.1 Regression-kriging . . . 38
2.4.3.2 Mean field bias . . . 39

Chapter 3: Results and Discussion **40**
3.1 Results . . . 40
3.1.1 Validation of Satellite-Based Precipitation Datasets . . . 40
3.1.1.1 Validation at daily time scale . . . 40
3.1.1.2 Validation at monthly time scale . . . 44
3.1.2 Bias Adjustment of Satellite-Based Precipitation Datasets . . . 47
3.1.2.1 Analysis of bias adjustment methods for daily rainfall accumulations . . . 47
3.1.2.2 Analysis of bias adjustment methods for monthly rainfall accumulations . . . 50
3.1.3 Merging of Satellite-Based Precipitation Datasets . . . 51

3.1.3.1 Analysis of merging methods for daily Datasets 51
3.1.3.2 Analysis of merging methods for monthly datasets 55
3.1.4 Summary of the main results of the study 58
3.2 Discussion 58

Bibliography **63**

Appendix **I**

Table of Contents **VI**